Relic gravitons and non-stationary processes

Massimo Giovannini [1]

Department of Physics, CERN, 1211 Geneva 23, Switzerland

INFN, Section of Milan-Bicocca, 20126 Milan, Italy

Abstract

Stationary processes do not accurately describe the diffuse backgrounds of relic gravitons whose correlations are homogeneous in space (i.e. only dependent upon the distance between the two spatial locations) but not in time. The symmetries of the autocorrelations ultimately reflect the quantum mechanical origin of the diffuse backgrounds and lead to non-stationary observables at late time. In particular, large oscillations are believed to arise in the spectral energy density that is customarily (but approximately) related to the tensor power spectrum. When the full expression of the spectral energy density is employed the amplitudes of oscillation are instead suppressed in the large-scale limit and the non-stationary features of the late-time signal practically disappear. For similar reasons the relations between the spectral energy density and the spectral amplitude are ambiguous in the presence of non-stationary features. While it is debatable if the non-stationary features are (or will be) directly detectable, we argue that the spectral amplitude following from the Wiener-Khintchine theorem is generally inappropriate for a consistent description of the relic signal. Nevertheless the strong oscillatory behaviour of the late-time observables is naturally smeared out provided the spectral energy density is selected as pivotal variable.

---

[1]e-mail address: massimo.giovannini@cern.ch

1 Introduction

The relic gravitational waves produced by the early variation of the space-time curvature [1–4] lead to a late-time background of diffuse radiation. In the simplest situation the relic gravitons are produced in pairs of opposite three-momenta from the inflationary vacuum and this is why they appear as a collection of standing (random) waves which are the tensor analog of the so-called Sakharov oscillations [5]; this phenomenon has been also independently discussed in the classic paper of Peebles and Yu [6] (see also [7]). The question analyzed in this paper involves the possibility of describing the relic gravitons in terms of a stationary and homogeneous stochastic process. As we shall see the answer to this question depends, to some extent, on the pivotal variable that is selected for the physical description of the relic graviton background.

A first general observation relevant in this context is that the late-time properties of the signal not only rest on the features of the inflationary vacuum but also on the post-inflationary evolution. It is well established that in the concordance paradigm the spectral energy density at late times is quasi-flat [8–10] and it is maximized in the aHz region[2] [11, 12] where the current Cosmic Microwave Background (CMB) observations are now setting stringent limits on the contribution of the relic gravitons to the temperature and polarization anisotropies [13–15]. The low-frequency constraints can be viewed as direct bounds on the tensor to scalar ratio r_T and seem to suggest that at higher frequencies (i.e. in the audio band and beyond) the spectral energy density in critical units should be $\mathcal{O}(10^{-17})$ or even smaller. The minuteness of the spectral energy density is however based on the presumption that radiation dominates (almost) right after the end of inflation and it is otherwise invalid [16]. The post-inflationary evolution prior to BBN nucleosynthesis is not probed by any direct observation and it can deviate from the radiation dominated evolution; if this is the case, it has been argued long ago that the high-frequency spectrum of the relic gravitons can be much larger [16] (see also Ref. [17] for a recent review). Even though the detectability of the signal is essential, for the present ends what matters are mainly the symmetries of the correlation functions.

The second general remark is that, at the moment, the direct observations that are potentially relevant for the relic graviton backgrounds involve the pulsar timing arrays (PTA) in the nHz range [18–21] and the ground-based interferometers [22, 23] operating in the audio band. It is actually well established since the late 1970s that the millisecond pulsars can be employed as effective detectors of random gravitational waves for a typical frequency domain that corresponds to the inverse of the observation time during which the pulsar timing has been monitored (see e.g. [24–26]). The correlation signature of an isotropic and random gravitational wave background should follow the so-called Hellings-Downs[3] curve [26]. A particularly interesting aspect, for the present purposes, involves the time-dependence of the signal suggested in [18]. At much higher frequencies the wide-band detectors are now setting bounds on the diffuse backgrounds of gravitational radiation between few Hz and 10 kHz. Since the late 1990s these bounds have been

---

[2]As usual we employ the prefixes of the international system of units so that, for instance, $1\,\mathrm{aHz} = 10^{-18}$ Hz, $1\,\mathrm{nHz} = 10^{-9}$ Hz and so on and so forth.

[3]In case the gravitational waves *are not* characterized by stochastically distributed Fourier amplitudes the corresponding signal does not necessarily follow the Hellings-Downs correlation. The previous data releases of the PTAs did not report specific evidence on the Hellings-Downs correlation [29–32]. The last data releases seem to suggest more compelling evidences [18–21] even if two competing experiments [18, 19] make slightly different statements on the Hellings-Downs correlation.

greatly improving and are now broadly compatible both with the PTA observations and with the big-bang nucleosynthesis constraints [33–35]. In the future it would be interesting to have detectors of relic gravitons operating directly in the MHz or GHz regions [36–39, 41–46] where direct bounds on relic gravitons are essential for determining the early expansion history of the Universe [47].

All in all, taking into account the considerations of the two previous paragraphs, the current searches of diffuse backgrounds of gravitational radiation assume that signal is in fact described by a stationary stochastic process characterized by a time-independent spectral amplitude [48, 49]. In this approach the correlation functions of the signal at different instants depend on the difference between the two times at which the random fields are evaluated so that the spectral amplitude is simply given by the Fourier transform of the autocorrelation function [50, 51]. As far as the spatial dependence is concerned the stochastic process is usually assumed to be homogeneous; by this we mean, according to the usual terminology, that the ensemble averages of the random fields evaluated at two different points depend on the distance between the two points. If the relic gravitons are produced from the quantum fluctuations of the gravitational field the homogeneity of the process is natural but not its stationarity.

The production of relic gravitons stipulates that the initial quantum state has evolved into a correlated multiparticle state [52]. As a consequence, in the Heisenberg description the field operators exhibit a characteristic pattern of non-stationary and standing oscillations which are in fact the tensor analog of the well known Sakharov oscillations [5]. When estimating the signal to noise ratio associated with the diffuse backgrounds of gravitational radiation the properties of the relic signal are assumed to be similar to the ones of the intrinsic noises of the detectors namely Gaussian, uncorrelated, stationary and statistically independent on the possible presence of other diffuse backgrounds [53–59]. In the first part of the present analysis, following some earlier observations [57,58] we shall first clarify that the relic graviton backgrounds are per se not equivalent to a stationary stochastic process since their autocorrelation function does not only depend on the time difference. In the second part of this investigation we shall present a number of specific examples. Finally in the third portion of the paper we shall analyze the variables where the non-stationary features are less pronounced. Contrary to a naive intuition we shall argue that the spectral amplitude is not appropriate for the description of a non-stationary signal while the spectral energy density is far more convenient. However the most heuristic approaches used for the estimate of the spectral energy density simply assume a well defined relation between the tensor power spectrum and the energy density without appreciating that such a relation is indeed approximate. As a consequence the spectral energy density exhibits late-time oscillations that are instead spurious. The best strategy for a direct evaluation of the spectral energy density is instead to impose the large-scale limit only after assessing all the relevant power spectra in their exact form. When this is properly done, the oscillations of the spectral energy density are suppressed in the large-scale limit and $\Omega_{gw}(\nu, \tau)$ turns out to be quasi-stationary; by this we mean that the strong oscillations do not arise to leading order but only in the corrections that are irrelevant for all the wavelengths shorter than the Hubble radius.

The layout of the paper is, in short, the following. In section 2 the stochastic processes are swiftly introduced with a particular focus on the tensor random fields. In section 3 we discuss the case of the relic gravitons and demonstrate that they cannot be reduced to the case of a stationary random process discussed in section 2. For this purpose the correlation functions are defined in terms of the appropriate quantum field operators. In section 4 the late-time autocorrelation functions are evaluated in two physically

significant cases: namely the situations where the universe is dominated by radiation and dusty matter. In section 5 we analyze the physical features of the spectral energy density and show that the order 1 oscillations are not a consequence of the non-stationary nature of the diffuse background but rather of the approximation scheme. We then compute exactly the spectral energy density in all the physical situations exemplified in section 4 and conclude that the spectral energy density only contains oscillating corrections that are suppressed in the large-scale limit. At the end of section 5 the spectral amplitude and the chirp amplitude are more specifically considered. The concluding remarks are collected in section 6. We found useful to relegate to the appendix a number of relevant technical discussions that could otherwise look as unwanted digressions in the bulk of the paper. In particular we discussed in appendix A the case of scalar random fields; appendix B is instead devoted to the explicit forms of the transition matrices that are employed in sections 4 and 5.

2   Stationary and non-stationary stochastic processes

The autocorrelation function of a *stationary* random process only depends upon the difference between the times at which the random fields of the ensemble average are evaluated [48,49]. The autocorrelation function must the be invariant under a common shift of the time coordinate and, for this reason, its Fourier transform is associated with a well defined spectral amplitude [50,51]. A stochastic process is instead *homogeneous* when the correlations of the relevant random fields evaluated at different points only depend upon the distance between the two spatial coordinates. Both stationarity and homogeneity play an important role when analyzing the correlation between gravitational wave detectors of arbitrary geometry [53–56]. In particular the intrinsic noises of the instruments are customarily assumed to be stationary, Gaussian, uncorrelated, much larger in amplitude than the gravitational strain, and statistically independent on the strain itself. The stationarity and the homogeneity are also conjectured for the signals associated with the diffuse background of gravitational radiation [59]. In what follows, after presenting the stationarity in the case of an ensemble of random functions, we consider the case of tensor random fields. To avoid digressions the results of the scalar case (employed in some of the derivations of this section) have been collected in the appendix A.

2.1   Random functions and stationary processes

Let us consider, for the sake of simplicity, an ensemble of real random functions $q(\tau)$ where τ denotes throughout the (conformal) time coordinate of the problem even if in this section the accurate identification of τ will not be essential[4]. With these specifications, the autocorrelation function can be defined in the context of the generalized harmonic analysis and its existence is associated with the finiteness of the integral [48]

$$\Gamma_q(\Delta\tau) = \lim_{T\to\infty} \frac{1}{2T} \int_{-T}^{T} q(\tau)q(\tau + \Delta\tau)\, d\tau, \tag{2.1}$$

---

[4]In this section the curvature of the space-time does not play any role. However, to avoid confusions, τ denotes throughout the conformal time coordinate. The background geometry will then be assumed to be conformally flat and characterized by a scale factor $a(\tau)$ so that the relations between the cosmic and the conformal time coordinates is given by $a(\tau)d\tau = dt$.

defined in the Lebesgue sense. The expression pf Eq. (2.1) applies in the case of a single function $q(\tau)$ and does not refer to any statistical concept. When dealing with a stationary and ergodic ensemble of random functions, the autocorrelation of Eq. (2.1) can be raplaced by

$$\Gamma_q(|\tau_1 - \tau_2|) = \langle\, q(\tau_1)\, q(\tau_2)\,\rangle, \tag{2.2}$$

where now $\langle\ldots\rangle$ now denotes an ensemble average whose result coincides, by definition, with Eq. (2.1) because of the hypotheses of ergodicity and stationarity. As we shall see later on in this section Eqs. (2.1)–(2.2) are easily generalized to the case of a stochastic quantum field. The Fourier transform of the autocorrelation function is ($S_q(\nu)$ in what follows) is, by definition, the spectral amplitude of the process:

$$q(\tau) = \int_{-\infty}^{+\infty} e^{2\,i\,\pi\,\nu\,\tau} q(\nu)\, d\nu, \qquad \langle q(\nu)\, q(\nu')\rangle = \delta(\nu + \nu')\, S_q(\nu), \tag{2.3}$$

where ν is the frequency[5]. The autocorrelation function and the spectral amplitudes are then related as

$$\Gamma_q(\tau_1 - \tau_2) = \frac{1}{2\pi} \int_{-\infty}^{\infty} e^{i\omega(\tau_1 - \tau_2)} S_q(\omega) d\omega = \int_{-\infty}^{\infty} e^{i\nu(\tau_1 - \tau_2)} S_q(\nu)\, d\nu. \tag{2.4}$$

According to Eq. (2.4) the spectral amplitude and the autocorrelation function of the process form a Fourier transform pair; this statement is often referred to as Wiener-Khintchine (see e.g. [49]) theorem and was originally developed in the framework of the so-called generalized harmonic analysis that establishes a rigorous connection between Eqs. (2.1) and (2.2) [50, 51]. The possibility of defining a spectral amplitude relies on the stationary nature of the underlying random process. The nomenclature employed hereunder is the one established in Eq. (2.4) and we shall call $S_q(\nu)$ *spectral amplitude*. There are however other terminologies: some authors call $S_q(\nu)$ *spectral density* or even power spectrum. For the sake of accuracy we stress that, in the present context, the power spectrum can be related to $S_q(\nu)$ in the case of a stationary process but it is, generally speaking, a different quantity. In particular the power spectrum defined hereunder is dimensionless whereas the spectral amplitude $S_q(\nu)$ has dimensions of an inverse frequency (or of a time).

2.2 Tensor random fields

2.2.1 Stationary processes

A solenoidal (and traceless) tensor random field can be treated with the same strategy already introduced in the scalar case. In particular the tensor amplitude can be transformed as

$$h_{ij}(\vec{x}, \tau) = \int_{-\infty}^{\infty} d\nu \int d\widehat{k}\, e^{2\,i\,\pi\,\nu\,(\tau - \widehat{k}\cdot\vec{x})}\, h_{ij}(\nu, \widehat{k}), \tag{2.5}$$

where $h_{ij}^*(\nu, \widehat{k}) = h_{ij}(-\nu, \widehat{k})$ and ν denotes, as usual, the comoving frequency. The tensor amplitude $h_{ij}(\nu, \widehat{k})$ can be expanded in the basis of the linear polarizations. As usual we introduce three orthogonal

---

[5]We shall use throughout the natural units $\hbar = c = 1$; this means, in particular, that $\omega = k = 2\pi\,\nu$ where ν is the frequency and ω the angular frequency. Occasionally in the literature involving the diffuse backgrounds of gravitational radiation the frequency ν is also denoted by f (see e.g. [59]) but we shall not use this notation that would be ambiguous in the present context.

unit vectors $\hat{m}$, $\hat{n}$ and $\hat{k}$ so that the two tensor polarizations as $e_{ij}^{\oplus} = (\hat{m}_i\,\hat{m}_j - \hat{n}_i\,\hat{n}_j)$ and $e_{ij}^{\otimes} = (\hat{m}_i\,\hat{n}_j + \hat{n}_i\,\hat{m}_j)$. With these standard notations we can write

$$h_{ij}(\nu,\widehat{k}) = \sum_{\lambda=\oplus,\,\otimes} e_{ij}^{(\lambda)}(\widehat{k})\,h_\lambda(\nu,\widehat{k}). \tag{2.6}$$

In analogy with the scalar case $S_h(\nu)$ is introduced from the expectation value of the tensor amplitudes expressed as a function of ν and $\widehat{k}$:

$$\langle h_\lambda(\nu,\,\widehat{k})\,h_{\lambda'}(\nu',\,\widehat{k}')\rangle = \mathscr{C}_h\,S_h(\nu)\,\delta(\nu+\nu')\,\delta^{(2)}(\widehat{k}-\widehat{k}')\,\delta_{\lambda\,\lambda'}, \tag{2.7}$$

where $\mathscr{C}_h$ is an overall constant that plays the same role of $\mathscr{C}_\phi$ introduced in the scalar case. From Eq. (2.7) the autocorrelation function $\Gamma_h(\tau_1-\tau_2)$ is introduced from:

$$\langle h_\lambda(\widehat{k},\tau_1)\,h_{\lambda'}(\widehat{p},\tau_2)\rangle = \mathscr{C}_h\,\delta_{\lambda\lambda'}\,\delta^{(2)}(\widehat{k}-\widehat{p})\,\Gamma_h(\tau_1-\tau_2). \tag{2.8}$$

Ultimately the connection between the spectral amplitude $S_h(\nu)$ and the autocorrelation function $\Gamma_h(\tau_1-\tau_2)$ is given by:

$$S_h(\nu) = \int_{-\infty}^{\infty} e^{2\,i\,\nu\,z}\,\Gamma_h(z)\,dz, \tag{2.9}$$

in full analogy with the scalar case of Eq. (A.3). We can finally evaluate the expectation value of two tensor amplitudes with different indices; from Eqs. (2.6)–(2.7) we obtain:

$$\langle h_{ij}(\nu,\widehat{k})\,h_{\ell m}(\nu',\widehat{k}')\rangle = 4\mathscr{C}_h\mathscr{S}_{ijmn}(\hat{k})S_h(\nu)\,\delta^{(2)}(\widehat{k}-\widehat{k}')\,\delta(\nu+\nu'). \tag{2.10}$$

In Eq. (2.10) the sum over the polarizations has been expressed in terms of $\mathscr{S}_{ijmn}$

$$\mathscr{S}_{ijmn} = [p_{im}(\hat{k})p_{jn}(\hat{k}) + p_{in}(\hat{k})p_{jm}(\hat{k}) - p_{ij}(\hat{k})p_{mn}(\hat{k})]/4. \tag{2.11}$$

where, as usual, $p_{ij}(\hat{k}) = (\delta_{ij} - \widehat{k}_i\,\widehat{k}_j)$ denotes the transverse projector.

2.2.2 Homogeneous processes

Using Eq. (2.10) and the observation that $\mathscr{S}_{ijij} = 1$, the expectation value of the tensor amplitudes at equal time becomes

$$\langle h_{ij}(\vec{x},\tau)\,h^{ij}(\vec{x}+\vec{r},\tau)\rangle = 32\,\pi\,\mathscr{C}_h \int_0^{\infty} d\nu\,S_h(|\nu|)\,j_0(2\pi\,|\nu|\,r). \tag{2.12}$$

The same strategy illustrated in the scalar case suggests that the Fourier amplitudes of the tensor modes can be related to the tensor power spectrum conventionally denoted by $P_T(k,\tau)$. For this purpose we write

$$h_{ij}(\vec{x},\tau) = \frac{1}{(2\pi)^{3/2}} \int d^3k e^{-i\,\vec{k}\cdot\vec{x}}\,\overline{h}_{ij}(\vec{k},\tau), \qquad \overline{h}_{ij}(\vec{k},\tau) = \overline{h}_{ij}^*(-\vec{k},\tau). \tag{2.13}$$

In analogy with the scalar case, for a homogeneous stochastic process the Fourier amplitudes obey

$$\langle \overline{h}_{ij}(\vec{k},\tau)\,\overline{h}_{mn}(\vec{p},\tau)\rangle = \frac{2\pi^2}{k^3}\delta^{(3)}(\vec{k}+\vec{p})P_T(k,\tau)\mathscr{S}_{ijmn}(\hat{k}). \tag{2.14}$$

6

It then follows that the expectation value of the quadratic combination $h_{ij}(\vec{x}, \tau) \, h^{ij}(\vec{x} + \vec{r}, \tau)$ can be written in two different ways depending the expansion we use; but since both expansions refer to the same tensor random field they must ultimately coincide so that

$$\langle \, h_{ij}(\vec{x}, \tau) \, h^{ij}(\vec{x} + \vec{r}, \tau) \, \rangle = 32 \, \pi \, \mathscr{C}_h \int_0^\infty d\nu \, S_h(|\nu|) \, j_0(2\pi \, |\nu| \, r) = \int_0^\infty \frac{d \, k}{k} P_T(k, \tau) \, j_0(k \, r). \tag{2.15}$$

Again, provided the tensor power spectrum is truly stationary we can then relate $P_T(k)$ to the spectral amplitude with the result that, as expected,

$$\nu \, S_h(|\nu|) = P_T(\nu), \qquad 32 \, \pi \, \mathscr{C}_h = 1, \tag{2.16}$$

where the difference between the condition appearing in Eq. (A.10) comes from the sum over the polarizations. As in the scalar case, the connection between the spectral amplitude and the tensor power spectrum obtained in Eq. (2.16) is only rigorous when the stochastic process is *both* stationary and homogeneous.

3 The relic gravitons and their quantum correlations

3.1 Stochastic processes and quantum expectation values

In a conformally flat background geometry chracterized by a scale factor $a(\tau)$ (where τ now denotes the conformal time coordinate) the tensor modes of the geometry may be amplified from their quantum mechanical fluctuations [1–4]. For the sake of illustration we shall be considering an inflationary stage possibly followed by the standard post-inflationary evolution [8–12]. When the scalar and tensor modes of the geometry are amplified from there quantum fluctuations (see, for instance, [17]) the random fields introduced in section 2 must be replaced by the appropriate field operators $\widehat{h}_{ij}(\vec{x}, \tau)$ that are solenoidal (i.e. $\partial_i \, \widehat{h}^i_j = 0$) and traceless (i.e. $\widehat{h}^i_i = 0$). The expectation values of these field operators in Fourier space define the tensor power spectrum

$$\langle \widehat{h}_{ij}(\vec{k}, \tau) \, \widehat{h}_{mn}(\vec{p}, \tau) \rangle = \frac{2\pi^2}{k^3} \, \mathcal{S}_{ijmn}(\hat{k}) P_T(k, \tau) \, \delta^{(3)}(\vec{k} + \vec{p}), \tag{3.1}$$

which is in fact the analog of Eq. (2.14) with the difference that its specific form now depends on the mode functions of the quantum field. The expectation value of the tensor amplitude must be complemented by the one of the corresponding time derivatives whose evolution cannot be neglected:

$$\langle \, \partial_\tau \widehat{h}_{ij}(\vec{k}, \tau) \, \partial_\tau \widehat{h}_{mn}(\vec{p}, \tau) \rangle = \frac{2\pi^2}{k^3} \, \mathcal{S}_{ijmn}(\hat{k}) Q_T(k, \tau) \, \delta^{(3)}(\vec{k} + \vec{p}). \tag{3.2}$$

where $Q_T(k, \tau)$ is the corresponding power spectrum. The explicit form of the field operators in the Heisenberg representation is:

$$\widehat{h}_{ij}(\vec{x}, \tau) = \frac{\sqrt{2} \, \ell_P}{(2\pi)^{3/2}} \sum_{\alpha = \oplus, \otimes} \int d^3 k \, e_{ij}^{(\alpha)}(\hat{k}) \left[F_{k,\alpha}(\tau) \, \widehat{b}_{\vec{k}, \alpha} e^{-i\vec{k}\cdot\vec{x}} + \text{H. c.} \right], \tag{3.3}$$

where $\ell_P = 8\pi G$ is the Planck length. In Eq. (3.3) the second term inside the square bracket denotes the Hermitian conjugate of the preceding one and the sum runs over the two orthogonal tensor polarizations

defined previously (see Eq. (2.5) and discussion thereafter). Sticking to the mode expansion of Eq. (3.3) the corresponding canonical momenta are given by[6]:

$$\widehat{\pi}_{ij}(\vec{x}, \tau) = \frac{a^2(\tau)}{4\sqrt{2}\, \ell_P\, (2\pi)^{3/2}} \sum_{\beta=\oplus,\otimes} \int d^3k\ e_{ij}^{(\beta)}(\hat{k}) \left[G_{k,\beta}(\tau)\, \widehat{b}_{\vec{k},\beta}\, e^{-i\vec{k}\cdot\vec{x}} + \mathrm{H.\,c.} \right], \tag{3.4}$$

where $a(\tau)$ is the scale factor; the mode functions for the momenta are $G_k = F_k'$ where the prime will denote, from now on, the derivation with respect to the conformal time coordinate τ. The Fourier transform of the Hermitian field operators of Eqs. (3.3)–(3.4) is then given by

$$\widehat{h}_{ij}(\vec{q}, \tau) = \sqrt{2}\, \ell_P \sum_\alpha \left[e_{ij}^{(\alpha)}(\hat{q})\, \widehat{b}_{\vec{q},\alpha}\, F_{q,\alpha}(\tau) + e_{ij}^{(\alpha)}(-\hat{q})\widehat{b}_{-\vec{q},\alpha}^\dagger F_{q,\alpha}^*(\tau) \right], \tag{3.5}$$

$$\widehat{\pi}_{mn}(\vec{p}, \tau) = \frac{a^2}{4\sqrt{2}\,\ell_P} \sum_\beta \left[e_{mn}^{(\beta)}(\hat{p})\, \widehat{b}_{\vec{p},\beta}\, G_{p,\beta}(\tau) + e_{mn}^{(\beta)}(-\hat{p})\widehat{b}_{-\vec{p},\beta}^\dagger G_{p,\beta}^*(\tau) \right]. \tag{3.6}$$

If we then impose canonical commutation relations between the field operators of Eqs. (3.5)–(3.6)

$$\left[\widehat{h}_{ij}(\vec{q}, \tau),\, \widehat{\pi}_{mn}(\vec{p}, \tau) \right] = i\, \mathcal{S}_{ijmn}(\hat{q})\, \delta^{(3)}(\vec{q} + \vec{p}), \tag{3.7}$$

must necessarily be normalized as:

$$F_q(\tau)\, G_q^*(\tau) - F_q^*(\tau) G_q(\tau) = i/a^2(\tau). \tag{3.8}$$

The condition expressed by Eq. (3.8) is essential to obtain the correct final expressions of the mode functions and it is verified throughout all the stages of the dynamical evolution.

3.2 Homogeneous processes and generalized autocorrelation functions

If the explicit expressions of Eqs. (3.5)–(3.6) are inserted into Eqs. (3.1)–(3.2) the two power spectra $P_T(k,\tau)$ and $Q_T(k,\tau)$ are given by:

$$P_T(k,\tau) = \frac{4\ell_P^2}{\pi^2}\, k^3\, |F_k(\tau)|^2, \qquad Q_T(k,\tau) = \frac{4\ell_P^2}{\pi^2}\, k^3\, |G_k(\tau)|^2. \tag{3.9}$$

The two-point functions associated with $P_T(k,\tau)$ and $Q_T(k,\tau)$ are in fact associated with homogeneous two-point functions of the type of Eq. (2.15)

$$\langle \widehat{h}_{ij}(\vec{x}, \tau)\, \widehat{h}^{ij}(\vec{x} + \vec{r}, \tau) \rangle = \int_0^\infty P_T(k, \tau)\, j_0(k\, r)\, \frac{dk}{k},$$

$$\langle \partial_\tau \widehat{h}_{ij}(\vec{x}, \tau)\, \partial_\tau \widehat{h}^{ij}(\vec{x} + \vec{r}, \tau) \rangle = \int_0^\infty Q_T(k, \tau)\, j_0(k\, r)\, \frac{dk}{k}. \tag{3.10}$$

To analyze the stationarity of the process we therefore need to introduce the autocorrelation functions that we define as:

$$\Gamma_{ijmn}(\vec{k}, \vec{p}, \tau_1, \tau_2) = \frac{1}{2} \left[\langle \widehat{h}_{ij}(\vec{k}, \tau_1)\, \widehat{h}_{mn}(\vec{p}, \tau_2) \rangle + \langle \widehat{h}_{ij}(\vec{p}, \tau_2)\, \widehat{h}_{mn}(\vec{k}, \tau_1) \rangle \right], \tag{3.11}$$

$$\overline{\Gamma}_{ijmn}(\vec{k}, \vec{p}, \tau_1, \tau_2) = \frac{1}{2} \left[\langle \partial_{\tau_1} \widehat{h}_{ij}(\vec{k}, \tau_1)\, \partial_{\tau_2} \widehat{h}_{mn}(\vec{p}, \tau_2) \rangle + \langle \partial_{\tau_2} \widehat{h}_{ij}(\vec{p}, \tau_2)\, \partial_{\tau_1} \widehat{h}_{mn}(\vec{k}, \tau_1) \rangle \right]. \tag{3.12}$$

---

[6]Both $\widehat{h}_{ij}(\vec{x}, \tau)$ and $\widehat{\pi}_{ij}(\vec{x}, \tau)$ are Hermitian, i.e. $\widehat{h}_{ij}^\dagger(\vec{x}, \tau) = \widehat{h}_{ij}(\vec{x}, \tau)$ and $\widehat{\pi}_{ij}^\dagger(\vec{x}, \tau) = \widehat{\pi}_{ij}(\vec{x}, \tau)$.

From Eq. (3.3) we can deduce the the explicit expressions of $\widehat{h}_{ij}(\vec{k}, \tau)$ and then compute directly Eqs. (3.11)–(3.12) whose explicit form becomes

$$\Gamma_{ijmn}(\vec{k}, \vec{p}, \tau_1, \tau_2) = \mathcal{S}_{ijmn}(\hat{k}) \, \delta^{(3)}(\vec{k} + \vec{p}) \, \Delta_k(\tau_1, \tau_2), \tag{3.13}$$

$$\overline{\Gamma}_{ijmn}(\vec{k}, \vec{p}, \tau_1, \tau_2) = \mathcal{S}_{ijmn}(\hat{k}) \, \delta^{(3)}(\vec{k} + \vec{p}) \, \overline{\Delta}_k(\tau_1, \tau_2), \tag{3.14}$$

where $\Delta_k(\tau_1, \tau_2)$ and $\overline{\Delta}_k(\tau_1, \tau_2)$ are given by:

$$\Delta_k(\tau_1, \tau_2) = 4\ell_P^2 \Big[F_k(\tau_1) \, F_k^*(\tau_2) + F_k(\tau_2) \, F_k^*(\tau_1) \Big], \tag{3.15}$$

$$\overline{\Delta}_k(\tau_1, \tau_2) = 4\ell_P^2 \Big[G_k(\tau_1) \, G_k^*(\tau_2) + G_k(\tau_2) \, G_k^*(\tau_1) \Big]. \tag{3.16}$$

The evolution of the mode functions $F_k(\tau)$ and $G_k(\tau)$ follows immediately from the action of the problem

$$S_g = \frac{1}{8\ell_P^2} \int d^4x \, \sqrt{-\overline{g}} \, \partial_\mu h_{ij} \, \partial_\nu h^{ij}, \tag{3.17}$$

where $\overline{g}_{\mu\nu}$ is the background metric and $\overline{g}$ its determinant. In the conformally flat case $\overline{g}_{\mu\nu} = a^2(\tau) \, \eta_{\mu\nu}$ and the Hamiltonian operator associated with the classical action (3.17) is given by[7]:

$$\widehat{H}_g(\tau) = \int d^3x \left[\frac{8\ell_P^2}{a^2} \, \widehat{\pi}_{ij} \, \widehat{\pi}^{ij} + \frac{a^2}{8\ell_P^2} \, \partial_k \widehat{h}_{ij} \, \partial_k \widehat{h}^{ij} \right]. \tag{3.18}$$

From Eq. (3.18) the evolution equations of the field operators is then given by:

$$\partial_\tau \widehat{\pi}_{ij} = \frac{a^2}{8\ell_P^2} \nabla^2 \widehat{h}_{ij}, \qquad \partial_\tau \widehat{h}_{ij} = \frac{8\ell_P^2}{a^2} \, \widehat{\pi}^{ij}, \tag{3.19}$$

so that the corresponding mode functions obey:

$$G_k' + 2\mathcal{H} \, G_k = -k^2 \, F_k, \qquad G_k = F_k', \tag{3.20}$$

where $\mathcal{H} = a'/a$. During inflation we have that $\mathcal{H} = -1/[(1 - \epsilon)\tau]$ where $\epsilon = -\dot{H}/H^2$ is the standard slow-roll parameter. From the Wronskian normalization condition of Eq. (3.8) the solution of Eq. (3.20) during the inflationary stage is given by

$$F_k(\tau) = \frac{f_k}{a(\tau)} = \frac{\mathcal{N}}{\sqrt{2k} \, a(\tau)} \sqrt{-k\tau} \, H_\nu^{(1)}(-k\tau), \tag{3.21}$$

$$G_k(\tau) = \frac{\mathcal{N}}{a(\tau)} \sqrt{\frac{k}{2}} \left[-\frac{2\nu}{\sqrt{-k\tau}} H_\nu^{(1)}(-k\tau) + \sqrt{-k\tau} \, H_{\nu+1}^{(1)}(-k\tau) \right], \tag{3.22}$$

where $H_\nu^{(1)}(z)$ is the Hankel function of first order [60, 61] and $\nu = (3 - \epsilon)/[2(1 - \epsilon)]$ the Bessel index; note that in Eq. (3.22) $|\mathcal{N}| = \sqrt{\pi/2}$. The results of Eqs. (3.21)–(3.22) hold during a quasi-de Sitter stage of expansion taking place for $\tau < -\tau_r$, i.e. when the conformal time coordinate takes negative values; τ_r denotes, in this context the end of the inflationary stage and the onset of the decelerated phase. Thanks to the initial conditions of Eqs. (3.21)–(3.22) the autocorrelation functions (3.15)–(3.16) can then be estimated in the different stages of the post-inflationary evolution and this is the general theme of the following section.

---

[7]Since the problem is inherently time-dependent, different Hamiltonians (all related by canonical transformations) can be introduced even if, ultimately, the evolution of the field operators remains unaffected. The transformed Hamiltonians might however lead to slightly different initial vacua and different canonical momenta. These aspects have been discussed in various related frameworks (see e.g. [52]) but are not central to the present discussion.

4 The late-time values of the autocorrelation functions

The late-time autocorrelation functions can be evaluated by enforcing at any stage of the dynamical evolution the continuity of the background and the Wronskian normalization condition of Eq. (3.8). These two requirements preserve the canonical form of the commutation relations and ultimately lead to standing oscillations in the mode functions. The rationale for this peculiar behaviour is related to the production of pairs of gravitons (with opposite three momenta) from the inflationary vacuum. The presence of the standing waves at late time also implies that the autocorrelation function does not only depend on the time-difference $|\tau_1 - \tau_2|$, as as it would happen in the case of a stationary process of the kind examined in section 1. We are now going to analyze the explicit form of the autocorrelation functions in two relevant examples.

4.1 The radiation stage and the related autocorrelation functions

A smooth evolution of the extrinsic curvature of the background demands the continuity of the inflationary scale factor and of its first derivative across the transition to the radiation-dominated phase. It is practical to introduce the variable $u(\tau)$ accounting for the continuity of the mode functions and of the background geometry

$$u(\tau) = k\,[\tau + (2 - \epsilon)\tau_r], \qquad \tau > -\tau_r, \qquad \epsilon = -\dot{H}/H^2, \tag{4.1}$$

where τ_r conventionally denotes the onset of the radiation-dominated stage and ϵ is the standard slow-roll parameter; by definition $u_r = u(-\tau_r) = k(1 - \epsilon)\tau_r$. It is important to stress that Eq. (4.1) (as all the subsequent discussion) assumes a quasi-de Sitter evolution during inflation where, according to the consistency conditions, $\epsilon \simeq r_T/16$. Even if according to observational data $r_T < 0.03$ [13–15](and consequently $\epsilon < 0.001$) it is important to keep track of the solw-roll corrections since their presence guarantees the continuity of the mode functions and the enforcement of the Wronskian normalization condition. In terms of u and u_r the late-time values of $f_k(\tau)$ and $g_k(\tau)$ during the radiation stage can then be expressed in terms of a 2×2 transition matrix

$$
\begin{aligned}
f_k(\tau) &= A_{ff}^{(r)}(u,\,u_r)\overline{f}_k \,+\, A_{fg}^{(r)}(u,\,u_r)\,\overline{g}_k/k, \\
g_k(\tau) &= A_{gf}^{(r)}(u,\,u_r)k\,\overline{f}_k \,+\, A_{gg}^{(r)}(u,\,u_r)\overline{g}_k,
\end{aligned}
\tag{4.2}
$$

where, for the sake of convenience, the mode functions have been rescaled as $F_k(\tau) = f_k(\tau)/a(\tau)$ and $G_k(\tau) = g_k(\tau)/a(\tau)$. The results holding in for a radiation stage can be easily generalized to any expanding stage; we also note that the various entries of the transition matrix are all real and they are explicitly given in the appendix B together with their limits. The values of $\overline{f}_k \equiv f_k(-\tau_r)$ and $\overline{g}_k \equiv g_k(-\tau_r)$ are fixed by the mode functions evaluated at the end of inflation (i.e. for $\tau = -\tau_r$) and are explicitly given by

$$\overline{f}_k = \frac{\mathcal{N}}{\sqrt{2k}}\,\sqrt{k\tau_r}\,H_\nu^{(1)}(k\tau_r), \qquad \overline{g}_k = \mathcal{N}\sqrt{\frac{k}{2}}\left[-\frac{2\,\nu}{\sqrt{k\tau_r}}H_\nu^{(1)}(k\tau_r) + \sqrt{k\tau_r}\,H_{\nu+1}^{(1)}(k\tau_r)\right]. \tag{4.3}$$

As discussed in mode detail in appendix B the general condition of Eq. (3.8) demands that the transition matrix is unitary i.e.

$$A_{ff}^{(r)}(u,\,u_r)\,A_{gg}^{(r)}(u,\,u_r) \,-\, A_{fg}^{(r)}(u,\,u_r)\,A_{gf}^{(r)}(u,\,u_r) = 1. \tag{4.4}$$

The condition (4.4) is written in a particular case but it is obviously a general property that must be enforced for any continuous transition of the background geometry; see also, in this respect, the discussion after Eq. (B.4). Let us now consider the modes that reentered the Hubble radius during radiation[8]. The mode functions of Eq. (4.2) can be expressed in the following form

$$f_k(\tau) = A_{ff}^{(r)}(u, u_r) \, \overline{f}_k \left[1 + \frac{A_{fg}^{(r)}(u, u_r)}{A_{ff}^{(r)}(u, u_r)} \left(\frac{\overline{g}_k}{k \, \overline{f}_k} \right) \right],$$

$$g_k(\tau) = A_{gf}^{(r)}(u, u_r) \, \overline{f}_k \left[1 + \frac{A_{gg}^{(r)}(u, u_r)}{A_{gf}^{(r)}(u, u_r)} \left(\frac{\overline{g}_k}{k \, \overline{f}_k} \right) \right], \tag{4.5}$$

where the second term appearing inside each of the squared brackets of Eq. (4.5) is always subleading in the limit $|u_r| \ll 1$, i.e. when the relevant wavelengths are all shorter than the Hubble radius for $\tau > -\tau_r$. Thanks to Eq. (4.5) and bearing in mind the results of Eqs. (B.1)–(B.2) the mode functions $F_k(u)$ and $G_k(u)$ are explicitly given by:

$$F_k(u) = \overline{F}_k^{(r)} j_0(u) \left[1 + \mathcal{O}(u_r^2) \right], \qquad G_k(u) = -k \, \overline{F}_k^{(r)} j_1(u) \left[1 + \mathcal{O}(u_r^2) \right], \tag{4.6}$$

where $j_0(u)$ and $j_1(u)$ denote the (spherical) Bessel functions of order 0 and 1 respectively [60, 61]. The amplitude of the mode functions $\overline{F}_k^{(r)}$ determines the amplitude of the tensor power spectrum during inflation for typical wavelengths larger than the Hubble radius, i.e.

$$\overline{P}_T^{(r)} = \frac{16}{\pi} \left(\frac{H_r}{M_P} \right)^2 \left(\frac{k}{a_r \, H_r} \right)^{n_T} = \frac{128}{3} \left(\frac{V}{M_P^4} \right)_{k \simeq H_r a_r}, \tag{4.7}$$

where we defined, for the sake of conciseness, $\overline{P}_T^{(r)} = \overline{P}_T(k, \tau_r)$ and $n_T = -2\epsilon = -r_T/8$. In Eq. (4.7) V denotes the inflationary potential which is related to the expansion rate in the slow-roll approximation $3 H^2 \overline{M}_P^2 \simeq V$; as already mentioned prior to Eq. (4.5) and in the related footnote H_r is, roughly speaking, the expansion rat at the end of inflation. Note finally that M_P (appearing in Eq. (4.7)), $\overline{M}_P$ and ℓ_P (introduced in Eq. (4.11)) are all related as $\overline{M}_P = \ell_P^{-1} = M_P/\sqrt{8\pi}$. All in all the autocorrelation functions of Eqs. (3.13)–(3.14) and (3.15)–(3.16) can be directly expressed in terms of $\overline{P}_T^{(r)}$

$$\Delta_k(\tau_1, \tau_2) = \frac{\pi^2 \, \overline{P}_T^{(r)}}{k^3} \frac{[\cos(u_1 - u_2) - \cos(u_1 + u_2)]}{u_1 u_2}, \tag{4.8}$$

$$\overline{\Delta}_k(\tau_1, \tau_2) = \frac{\pi^2 \, \overline{P}_T^{(r)}}{k} \left[\frac{\cos(u_1 - u_2)}{u_1 u_2} \left(1 + \frac{1}{u_1 u_2} \right) + \frac{\sin(u_1 - u_2)}{u_1 u_2} \left(\frac{1}{u_2} - \frac{1}{u_1} \right) \right.$$

$$+ \left. \frac{\cos(u_1 + u_2)}{u_1 u_2} \left(1 - \frac{1}{u_1 u_2} \right) - \frac{\sin(u_1 + u_2)}{u_1 u_2} \left(\frac{1}{u_2} + \frac{1}{u_1} \right) \right], \tag{4.9}$$

where, by definition, $u_1 = u(\tau_1)$ and $u_2 = u(\tau_2)$. But since at late-times $u_1 \simeq k\tau_1$ and $u_2 = k\tau_2$, the autocorrelation functions of Eqs. (3.11)–(3.12) do not only depend on the time difference, as implied in the case of stationary processes discussed in section 2. On the contrary both autocorrelation functions $\Delta_k(\tau_1, \tau_2)$ and $\overline{\Delta}_k(\tau_1, \tau_2)$ include terms depending both on $(\tau_1 - \tau_2)$ and on $(\tau_1 + \tau_2)$. There also a number of corrections going as inverse powers of u_1 and u_2; some of these corrections are suppressed when the wavelengths of the gravitons are much smaller than the Hubble radius during the radiation stage.

---

[8]In this case the continuity of the evolution of $a(\tau)$ and $\mathcal{H}(\tau)$ implies that, during radiation, $a_r(\tau) = [\beta(\epsilon)(\tau/\tau_r) + \beta(\epsilon) + 1]$ where $\beta(\epsilon) = 1/(1 - \epsilon)$. During inflation, as usual, $a H = -\beta(\epsilon)/\tau]$ whereas, at the end of inflation (i.e. for $\tau \to -\tau_r$) $a_r H_r = \beta(\epsilon)/\tau_r$. Grossly speaking H_r denotes the expansion rate at the end of inflation.

4.2 The autocorrelation functions during the matter stage

The second relevant example involves the evolution during the matter stage. By enforcing at each stage of the evolution the Wronskian normalization of Eq. (3.8) (and the related canonical form of the commutation relations) the values of the mode functions during the matter stage are given by

$$
f_k(\tau) = A_{ff}^{(m)}(v,\, v_{eq})\, \overline{f}_k^{(m)} \left[1 + \frac{A_{fg}^{(m)}(v,\, v_{eq})}{A_{ff}^{(m)}(v,\, v_{eq})} \left(\frac{\overline{g}_k^{(m)}}{k\, \overline{f}_k^{(m)}} \right) \right],
$$

$$
g_k(\tau) = A_{gf}^{(m)}(v,\, v_{eq})\, \overline{f}_k^{(m)} \left[1 + \frac{A_{gg}^{(m)}(v,\, v_{eq})}{A_{gf}^{(m)}(v,\, v_{eq})} \left(\frac{\overline{g}_k^{(m)}}{k\, \overline{f}_k^{(m)}} \right) \right]. \tag{4.10}
$$

In this case the elements of the transition matrix Eq. (4.10) have been listed in Eqs. (B.3)–(B.4). Moreover the expression of $v = v(\tau)$ is the dust analog[9] of $u(\tau)$ introduced in Eq. (4.1)

$$
v = v(\tau) = k[\tau + \tau_{eq} + 2(2 - \epsilon)\, \tau_r], \qquad \tau \gg \tau_{eq}. \tag{4.11}
$$

As in the case of u_r we use here the shorthand notation $v_{eq} = v(\tau_{eq})$. By definition $\overline{f}_k^{(m)}$ and $\overline{g}_k^{(m)}$ are the values of the mode functions at the end of the radiation stage. From Eq. (4.5) we then have:

$$
\overline{f}_k^{(m)} = A_{ff}^{(r)}(u_{eq},\, u_r)\, \overline{f}_k \left[1 + \frac{A_{fg}^{(r)}(u_{eq},\, u_r)}{A_{ff}^{(r)}(u_{eq},\, u_r)} \left(\frac{\overline{g}_k}{k\, \overline{f}_k} \right) \right],
$$

$$
\overline{g}_k^{(m)} = A_{gf}^{(r)}(u_{eq},\, u_r)\, \overline{f}_k \left[1 + \frac{A_{gg}^{(r)}(u_{eq},\, u_r)}{A_{gf}^{(r)}(u_{eq},\, u_r)} \left(\frac{\overline{g}_k}{k\, \overline{f}_k} \right) \right], \tag{4.12}
$$

where, recalling the expression of Eq. (4.1), $u_{eq} = u(\tau_{eq}) \simeq k\tau_{eq}$. As in the case of Eq. (4.5) the second term inside each of the squared brackets of Eq. (4.10) turns out to be subleading in the limit $|v_{eq}| \ll 1$ which is appropriate for all the wavelengths that are shorter than the Hubble radius during the dust stage. Using then the results of Eqs. (B.3)–(B.4) together with Eqs. (4.10)–(4.12) the evolution of the mode functions during the matter stage takes the form

$$
F_k(v) = -\overline{F}_k^{(m)} \frac{j_1(v)}{v} \left[1 + \mathcal{O}(u_r^2) + \mathcal{O}(v_{eq}^2) + \mathcal{O}(u_r\, v_{eq}) \right],
$$

$$
G_k(v) = \overline{G}_k^{(m)} \frac{j_2(v)}{v} \left[1 + \mathcal{O}(u_r^2) + \mathcal{O}(v_{eq}^2) + \mathcal{O}(u_r\, v_{eq}) \right], \tag{4.13}
$$

where $j_1(v)$ and $j_2(v)$ are, respectively, the spherical Bessel functions of order 1 and 2. Finally the tensor power spectra $P_T(k, \tau)$ and $Q_T(k, \tau)$ can be directly expressed in terms of $\overline{P}_T(k, \tau_r)$:

$$
P_T(k,\, v) = 9\, \overline{P}_T^{(r)} \left[\frac{\cos v}{v^2} - \frac{\sin v}{v^3} \right]^2, \tag{4.14}
$$

$$
Q_T(k,\, v) = 9\, k^2\, \overline{P}_T^{(r)} \left[3\frac{\sin v}{v^4} - \frac{\sin v}{v^2} - 3\frac{\cos v}{v^3} \right]^2, \tag{4.15}
$$

---

[9] The continuity of the scale factor and of its first conformal time derivative implies $a(\tau) = \{\beta(\epsilon)(\tau + \tau_{eq}) + 2[\beta(\epsilon) + 1]\tau_r\}^2 / \{4\tau_r[\beta(\epsilon)\tau_{eq} + (\beta(\epsilon) + 1)\tau_r]\}$ for $\tau \geq \tau_{eq}$.

implying that, in the limit $v \ll 1$, $P_T(k, v) \to \overline{P}_T(k, \tau_r)$ and $Q_T(k, v) \to k^2 \overline{P}_T(k, \tau_r)$. The autocorrelation functions of Eqs. (3.15)–(3.16) can therefore be expressed as

$$
\begin{aligned}
\Delta_k(\tau_1, \tau_2) &= \frac{9\pi^2}{k^3} \frac{\overline{P}_T(k, \tau_r)}{v_1^2 v_2^2} \left[\cos(v_1 - v_2)\left(1 + \frac{1}{v_1 v_2}\right) + \sin(v_1 - v_2)\left(\frac{1}{v_2} - \frac{1}{v_1}\right) \right. \\
&+ \left. \cos(v_1 + v_2)\left(1 - \frac{1}{v_1 v_2}\right) - \sin(v_1 + v_2)\left(\frac{1}{v_2} + \frac{1}{v_1}\right) \right],
\end{aligned}
\tag{4.16}
$$

$$
\begin{aligned}
\overline{\Delta}_k(\tau_1, \tau_2) &= \frac{9\pi^2}{k} \frac{\overline{P}_T(k, \tau_r)}{v_1^2 v_2^2} \left[\cos(v_1 - v_2) A_-(v_1, v_2) - \cos(v_1 + v_2) A_+(v_1, v_2) \right. \\
&+ \left. 3\sin(v_1 - v_2) B_-(v_1, v_2) + 3\sin(v_1 + v_2) B_+(v_1, v_2) \right].
\end{aligned}
\tag{4.17}
$$

In Eqs. (4.16)–(4.17) we use the notation $v_1 = v(\tau_1)$ and and $v_2 = v(\tau_2)$. Furthermore the functions $A_\pm(v_1, v_2)$ and $B_\pm(v_1, v_2)$ are defined as:

$$
A_\pm(v_1, v_2) = 1 - \frac{3}{v_1^2} - \frac{3}{v_2^2} + \frac{9}{v_1^2 v_2^2} \mp \frac{9}{v_1 v_2}, \qquad B_\pm(v_1, v_2) = \frac{1}{v_2}\left(1 - \frac{3}{v_1^2}\right) \pm \frac{1}{v_1}\left(1 - \frac{3}{v_2^2}\right).
\tag{4.18}
$$

As in the case of radiation, it is clear that the autocorrelation function does not simply depend on $(v_1 - v_2) = k(\tau_1 - \tau_2)$ but also on $(v_1 + v_2) = k[(\tau_1 + \tau_2) + 2\tau_{eq} + 4(2 - \epsilon)]$. Moreover there are terms containing inverse powers of v_1 and v_2 which are not necessarily suppressed. The two examples proposed in the present and in the previous subsections can be extended to a various complementary situations where the intermediate expansion history deviates from the radiation dominated evolution and the high-frequency signal can be potentially much larger than in the case of the concordance paradigm [62].

4.3 Asymptotic form of the autocorrelation functions

When the wavelengths are all inside the Hubble radius the expressions of the autocorrelation functions become simpler since all terms that are suppressed in the limit $u \gg 1$ and $v \gg 1$ can be neglected in the first approximation. In particular during the radiation dominated stage for $u_1 \simeq u_2 \gg 1$ the contributions of the cosines always dominates in Eqs. (4.8)–(4.9) so that

$$
\Delta_k(\tau_1, \tau_2) = \frac{\pi^2 \overline{P}_T^{(r)}}{k^3} \frac{[\cos(u_1 - u_2) - \cos(u_1 + u_2)]}{u_1 u_2},
\tag{4.19}
$$

$$
\overline{\Delta}_k(\tau_1, \tau_2) = \frac{\pi^2 \overline{P}_T^{(r)}}{k} \frac{[\cos(u_1 - u_2) + \cos(u_1 + u_2)]}{u_1 u_2},
\tag{4.20}
$$

where $(u_1 - u_2) = k(\tau_1 - \tau_2)$ and $(u_1 + u_2) = k[(\tau_1 + \tau_2) + 2(2 - \epsilon)\tau_r]$. During the dust-dominated epoch Eqs. (4.17)–(4.18) can be evaluated in the limit $v_1 \simeq v_2 \gg 1$ and the result is formally similar to the one of Eqs. (4.19)–(4.20) but with different phases:

$$
\Delta_k(\tau_1, \tau_2) = \frac{9\pi^2}{k^3} \frac{\overline{P}_T^{(r)}}{v_1^2 v_2^2} \left[\cos(v_1 - v_2) + \cos(v_1 + v_2) \right],
\tag{4.21}
$$

$$
\overline{\Delta}_k(\tau_1, \tau_2) = \frac{9\pi^2}{k} \frac{\overline{P}_T^{(r)}}{v_1^2 v_2^2} \left[\cos(v_1 - v_2) - \cos(v_1 + v_2) \right],
\tag{4.22}
$$

The results of Eqs. (4.19)–(4.20) and (4.21)–(4.22) demonstrate in explicit terms that a stationary stochastic process it is not equivalent, strictly speaking, to the random process that describes the relic gravitons at

13

late times. The reason for this lack of equivalence is related to the production mechanism: relic gravitons are produced in pairs of opposite three-momenta. This is why the mode functions are ultimately standing waves; as a consequence the autocorrelation functions are not invariant under a common shift of the time coordinate. The possibility of observing the non-stationary nature of the autocorrelation function has been previously considered in the literature (see [57, 58] and references therein) with particular attention to the frequency widow of wide-band interferometers. If the frequency falls in the audio band we have that $\mathcal{O}(100)$ Hz. Let us then consider the non-stationary contributions at the present time; the typical oscillation phase will be

$$v_1 + v_2 = k[(\tau_1 + \tau_2) + 2\tau_{eq} + 4(2 - \epsilon)\tau_r] = \mathcal{O}(\nu_{ref}/\nu_p), \tag{4.23}$$

where ν_{ref} is a certain reference frequency and $\nu_p = \mathcal{O}(10^{-18})$ Hz. Even if ν_{ref} is sufficiently small the oscillation is so strong that the the the contribution of $\cos{(v_1 + v_2)}$, possibly integrated over the instrumental window of sensitivity (e.g. between ν_r and a sufficiently close ν_{max}), vanishes in comparison with the stationary contribution oscillating as $\cos{(v_1 - v_2)}$. In spite of this argument a non-stationary dependence of the diffuse background may be easily explained in terms of a relic signal. It is therefore essential to understand more accurately how the non-stationary corrections impact on the observables and, in particular, on the spectral energy density in critical units.

5 The oscillations of the spectral energy

The spectral amplitude $S_h(\nu)$ is not a well defined pivotal variable for the description of the signal when the diffuse backgrounds are non-stationary. Following the discussion of section 2 and taking into account the results of section 4 it turns out that similar conclusions could hold also in the case of other widely employed quantities like the spectral energy density or the chirp amplitude. In spite of this generic expectation we are now going to argue that the spectral energy density, when correctly evaluated, is quasi-stationary since the strong oscillations (potentially present to leading order both in the power spectrum and in the chirp amplitude) are progressively more suppressed when the wavelengths of the gravitons become shorter than the Hubble radius at each corresponding epoch. For this purpose it is useful to remind that there are actually two complementary ways in which the spectral energy density is usually evaluated, at least by looking at the current literature:

- in the first case the power spectrum is estimated (either analytically or numerically by means of an appropriate transfer function[10]) and then related to the spectral energy density; this evaluation only requires the direct calculation of $P_T(k, \tau)$;

- the second option is to estimate independently the power spectra $P_T(k, \tau)$ and $Q_T(k, \tau)$, compute the spectral energy density and then study the various relevant limits; among them the most relevant for the present ends is the one where all the wavelengths of the spectrum are shorter than the Hubble radius at each corresponding epoch.

---

[10]The considerations reported here have a direct impact on the transfer functions that can be defined either for the tensor power spectrum [63,64] or directly in terms of the spectral energy density [65]. If the ultimate purpose is an accurate assessment of the spectral energy density, between the two strategies the latter is far more consistent than the former. Furthermore a direct numerical evaluation of the spectral energy density automatically smears the oscillations that are manually averaged when defining the transfer function with respect to the tensor power spectrum.

The first strategy turns out to be the limit of the second when the wavelengths are inside the Hubble radius but, as we shall see, the approximate expression where $\Omega_{gw}(k,\tau)$ only depends on $P_T(k,\tau)$ holds for the overall amplitude but not for the phases. This is why the first approach discussed above leads to an expression that is not stationary whereas the second one implies a result that is overall stationary (barring for the effects of the expansion of the background). The quasi-stationarity comes, on a technical ground, from the destructive interference of the respective phases associated with $P_T(k,\tau)$ and $Q_T(k,\tau)$. The approximate and the exact approaches will now be analyzed in detail with the purpose of showing that the latter is more rigorous than the former. The spectral energy density turns then out to be in practice, quasi-stationary and therefore particularly suitable for the description of the diffuse backgrounds of cosmic origin.

5.1 Approximate evaluation and its spurious oscillations

The heuristic strategy for the evaluation of the spectral energy density acknowledges that the spectral energy density is only determined by the tensor power spectrum $P_T(k,\tau)$ and that the phases of $P_T(k,\tau)$ coincide exactly with the ones of $\Omega_{gw}(k,\tau)$ according to

$$\Omega_{gw}(k,\tau) = \frac{k^2}{12\mathscr{H}^2}\, P_T(k,\tau) \equiv \frac{k^2}{a^2\, H^2} P_T(k,\tau), \qquad \left|\frac{k}{a\,H}\right| \gg 1. \tag{5.1}$$

Equation (5.1) admittedly holds when the wavelengths are all shorter than the Hubble radius (i.e. $k \gg a\,H$)but it also suggests that the strong oscillations of $P_T(k,\tau)$ are translated into the phases of $\Omega_{gw}(k,\tau)$. Let us now apply Eq. (5.1) to two illustrative examples. The first one involves the situation where the comoving wavelengths are all inside the Hubble radius during the radiation dominated stage. In this case
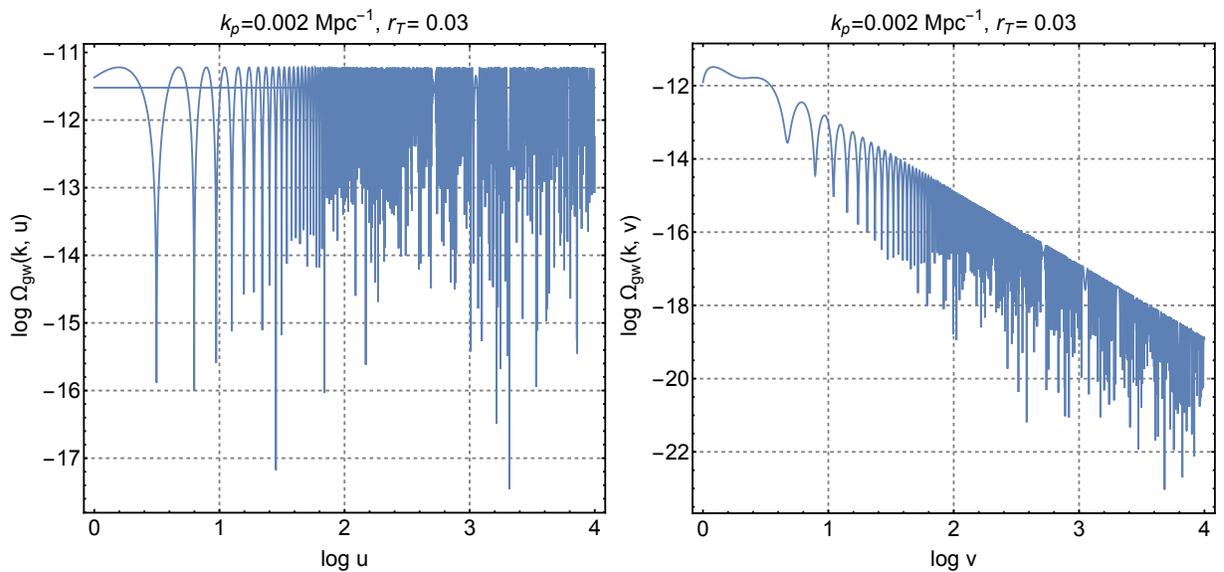

Figure 1: According to Eq. (5.2), the left plot we illustrate the common logarithm of $\Omega_{gw}(k,u)$ as a function of the common logarithm of u (see Eq. (4.11)). In the plot at the right we illustrate instead the common logarithm of $\Omega_{gw}(k,v)$ as a function of the common logarithm of v (see Eqs. (4.11) and (5.3)). Both results are a direct consequence of Eq. (5.1) which is, however, only approximate.

inserting Eq. (4.5) into Eq. (5.1) we obtain[11]

$$
\begin{aligned}
\Omega_{gw}(k, u) &= \frac{u^2}{12}\overline{P}_T^{(r)} \left| 1 + \frac{A_{fg}^{(r)}(u,\, u_r)}{A_{ff}^{(r)}(u,\, u_r)}\left(\frac{\overline{g}_k}{k\,\overline{f}_k}\right)\right|^2 \\
&= \frac{\overline{P}_T^{(r)}}{12}\sin^2 u\left[1 + \mathcal{O}(u_r^2)\right] \equiv \frac{\overline{P}_T^{(r)}}{12}\sin^2 u\left[1 + \mathcal{O}(u_r^2)\right] \simeq \frac{\overline{P}_T^{(r)}}{24}\,(1 - \cos 2u), \qquad u \gg 1, \text{ (5.2)}
\end{aligned}
$$

where $\overline{P}_T^{(r)}$ has been already defined in Eq. (4.7). The first equality in Eq. (5.2) follows from the exact result expressed in terms of the appropriate elements of the transition matrix (see also appendix B). Overall the result of Eq. (5.2) oscillates as $\sin^2 u$ up to terms $\mathcal{O}(u_r^2)$: these are in practice the scales that left the Hubble radius during inflation and reentered in the radiation stage (i.e. for $k\tau_r < 1$). To be even more accurate the result of Eq. (5.2) applies for $u \gg 1$ and $\tau \gg \tau_r$ so that, eventually, the two conditions are also equivalent to $k\tau \gg 1$ and $k \gg a H$. The second expression of Eq. (5.2) clearly follows from the first one by applying standard trigonometric identities and to artificially get rid of the oscillating contributions some authors just average the obtained result over an oscillation period even if this is, strictly speaking, an arbitrary procedure.

A further interesting example follows from the analysis of a dusty phase; if we actually insert the results of Eqs. (4.10) and (4.12) into Eq. (5.1) we obtain

$$
\Omega_{gw}(k, v) = \frac{3}{16\,v^2}\overline{P}_T^{(r)}\left(\cos^2 v + \frac{\sin^2 v}{v^2} - \frac{\sin 2v}{v^3}\right)\left[1 + \mathcal{O}(u_r^2) + \mathcal{O}(v_{eq}^2) + \mathcal{O}(u_r\,v_{eq})\right], \qquad v \gg 1. \qquad \text{(5.3)}
$$

As in the case of Eq. (5.2) the leading order result of Eq. (5.3) is strongly oscillating. In Fig. 1 we illustrate the results of Eqs. (5.2)–(5.3). We recall that the amplitudes of the spectral energy density is controlled by $\overline{P}_T^{(r)}$ which can be parametrized as $\mathcal{A}_T(k/k_p)^{n_T}$ where $k_p = 0.002\,\mathrm{Mpc}^{-1}$ is the pivot scale and $\mathcal{A}_T = r_T\,\mathcal{A}_{\mathcal{R}}$ the amplitude of the power spectrum. Since the tensor spectral index can be evaluated in terms of the consistency relations (i.e. $n_T = -r_T/8$) we can select, for instance, $r_T = 0.03$ (as suggested by the current data [13–15]). The results of Fig. 1 refer to the case $\mathcal{A}_{\mathcal{R}} = 2.41 \times 10^{-9}$ and for $k = \mathcal{O}(k_p)$. While we purposely employed realistic figures for the various parameters, we stress nonetheless that the obtained expressions of the spectral energy density are not of direct phenomenological applicability. To be accurate the equality transition and a number of late-time effects must be numerically discussed [52]. The full form of the spectral energy density that shall be discussed in the following subsection is also potentially relevant for the numerical applications [13, 14, 65].

5.2 Exact expression and the suppression of the oscillations

All in all we can summarize the results of the previous subsection by saying that Eq. (5.1) holds approximately only when the wavelengths are all much shorter than the Hubble radius. If the full form of the spectral energy density is instead adopted, the $\mathcal{O}(1)$ oscillations appearing in Fig. 1 practically disappear since they are suppressed for $k > a H$. Consequently their amplitude does not affect the leading term of the results and to clarify this point it is mandatory to start from a rigorous definition of the spectral energy

---

[11]It is important to stress that the result of Eq. (5.2) refers to the spectral energy density computed during the radiation-dominated stage and not at the present time. Similar comments hold also for other quantities discussed in this section (see e. g. Eq. (5.3)).
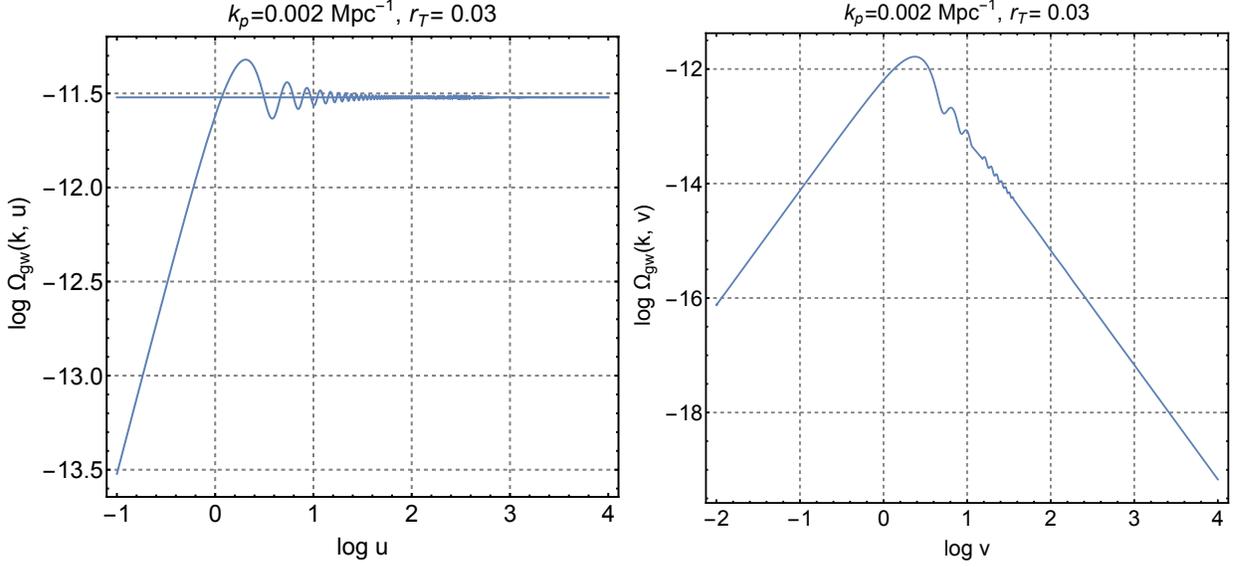
Figure 2: In the left plot we illustrate the common logarithm of $\Omega_{gw}(k, u)$ (given by Eq. (5.7)) as a function of the common logarithm of u. In the right plot we report instead the common logarithm of the expression given in Eq. (5.9) as a function of the common logarithm of v. The results of the two plots should be compared with Fig. 2 which reports exactly the same quantities but computed from the approximate expression of Eq. (5.1). As already stressed in connection with Eq. (5.2) the results reported here do not apply at the present time and neglect a number of important damping sources like the neutrino free-streaming, the evolution of the relativistic species and the transition to the dominance of dark energy; see, in this respect, the discussion at the end of subsection 5.2.

density. For this purpose the energy density must be introduced from the variation of Eq. (3.17) with respect to the background metric[12]; this procedure leads to a consistent energy-momentum pseudo-tensor of the relic gravitons [3, 4] (see also [66]):

$$T_{\alpha\beta}^{(gw)} = \frac{1}{4\ell_{\mathrm{P}}^2} \left[\partial_\alpha h_{ij} \, \partial_\beta h^{ij} - \frac{1}{2} \bar{g}_{\alpha\beta} \left(\bar{g}^{\mu\nu} \, \partial_\mu h_{ij} \, \partial_\nu h^{ij} \right) \right]. \tag{5.4}$$

In Eq. (5.4) the indices of $T_{\alpha\beta}^{(gw)}$ are raised and lowered with the help of the background metric (i.e. $T_{\alpha}^{(gw)\ \beta} = \bar{g}^{\beta\nu} T_{\alpha\nu}^{(gw)}$). Equation (3.17) implicitly assumes that the underlying background geometry is conformally flat so that in the case of a spatially flat Friedmann-Robertson-Walker metric $\bar{g}_{\mu\nu} = a^2(\tau)\, \eta_{\mu\nu}$ Eq. (5.4) leads directly to the energy-momentum tensor suggested by Ford and Parker [3,4] and the related energy density is [66]

$$\rho_{gw}(\vec{x}, \tau) = \frac{1}{8\, \ell_P^2\, a^2} \left(\partial_\tau h_{ij}\, \partial_\tau h^{ij} + \partial_m h_{ij} \partial^m h^{ij} \right). \tag{5.5}$$

If the field operators of Eqs. (3.1) and (3.3) are now inserted into Eq. (5.5) we can compute the expectation value $\langle \rho_{gw}(\vec{x}, \tau) \rangle$ so that the spectral energy density in critical units becomes:

$$\Omega_{gw}(k, \tau) = \frac{1}{\rho_{crit}} \frac{d\langle \rho_{gw} \rangle}{d\ln k} = \frac{1}{24\, H^2 a^2} \left[k^2 P_T(k, \tau) + Q_T(k, \tau) \right]. \tag{5.6}$$

---

[12]Different definitions of the energy-momentum pseudo-tensor lead however to the same conclusion. The way the spectral energy density is assigned is actually not unique and this relevant point will be discussed at the end of this section.

The evaluations of Eqs. (5.2)–(5.3) can now be repeated and compared with the results of Fig. 1. If we consider a radiation-dominated stage and insert the results of Eqs. (4.5)–(4.6) inside Eq. (5.6) we obtain:

$$\Omega_{gw}(k,\,u) = \frac{1}{24}\,\overline{P}_T^{(r)}\left(1 + \frac{\sin^2 u}{u^2} - \frac{\sin 2u}{u}\right). \tag{5.7}$$

The main difference between Eqs. (5.2) and (5.7) is that the former oscillates much more strongly than the latter. Furthermore while the expression of Eq. (5.7) applies both inside and outside the Hubble radius, Eq. (5.2) only applies when $u > 1$, i.e. for wavelengths shorter than the Hubble radius. For $\tau > \tau_r$ we have that, approximately, $u \simeq k\tau$ and when the wavelengths are shorter than the Hubble radius the spectral energy density is roughly constant up to oscillating corrections that are suppressed as $|k\tau|^{-1}$ and as $|k\,\tau|^{-2}$ in the limit $|k\tau| \gg 1$, i.e.

$$\Omega_{gw}^{(r)}(k,\tau_r,\tau) = \frac{\overline{P}_T(k,\tau_r)}{24}\left(1 + \mathcal{O}\left(\frac{1}{k\tau}\right) + \mathcal{O}\left(\frac{1}{k^2\tau^2}\right)\right), \qquad k\tau \gg 1. \tag{5.8}$$

From Eq. (5.1) the amplitude of oscillation is only determined from $P_T(k,\tau)$ but if we look at Eq. (5.6) we see that the the final results comes in fact from the mutual interference of $P_T(k,\tau)$ and $Q_T(k,\tau)$: while each of the terms is strongly oscillating their combination is quasi-stationary, as anticipated. The same
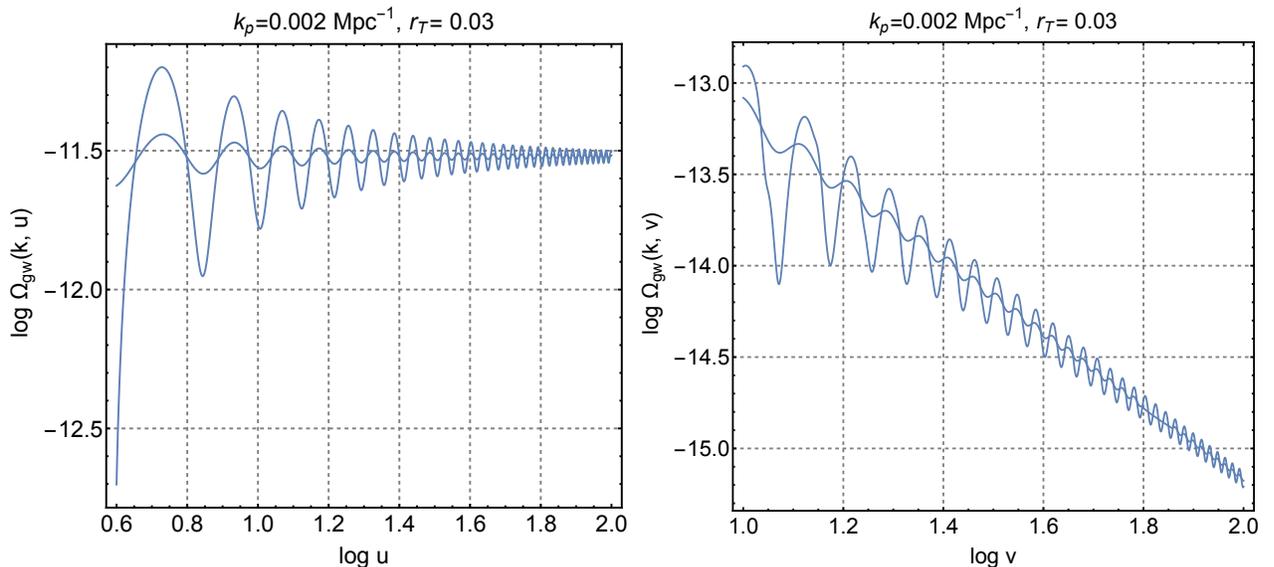

Figure 3: In the left plot the common logarithm of $\Omega_{gw}(k,u)$ (given by Eq. (5.7)) is illustrated as a function of the common logarithm of u. In the right plot we report instead the common logarithm of the expression given in Eq. (5.9) as a function of the common logarithm of v. The left and the right plots should be compared with Fig. 1 that illustrates the approximate expression of Eq. (5.1). In both plots the oscillations with the largest amplitude follow from Eqs. (5.7)–(5.9) while the ones with a comparatively smaller amplitude have been already given in Fig. 2. We therefore conclude that different definitions of the energy-momentum pseudo-tensor modulate the final result in a different way but always suppress the oscillations that would appear to leading order.

approach adopted in the derivation of Eqs. (5.7)–(5.8) can be applied during a dust-dominated stage with

the result that the spectral energy density becomes

$$\Omega_{gw}(v) = \frac{3\overline{P}_T^{(r)}}{32\,v^2}\left[1 + 2\frac{\sin 2v}{v} + \frac{9\cos^2 v - 5\sin^2 v}{v^2} - \frac{9\sin 2v}{v^3} + 9\frac{\sin^2 v}{v^4}\right].\tag{5.9}$$

As in the case of Eq. (5.8), also the result of Eq. (5.9) holds both for $v < 1$ and $v > 1$. Again, by comparing Eqs. (5.3) and (5.9) the strong oscillations of the leading term disappear and they get suppressed for $v \gg 1$. The results of Eqs. (5.8)–(5.9) depend on a pair of contributions coming, respectively, from $k^2 P_T(k,\tau)$ and $Q_T(k,\tau)$. The phases of oscillations appearing in Eq. (5.8) are controlled by the combination $[j_0^2(u) + j_1^2(u)]$ (where, as usual, $j_0(u)$ and $j_1(u)$ are the spherical Bessel functions). When $u \gg 1$ we have that $j_0^2(u) \simeq j_1^2(u)$ so that we may replace $[j_0^2(u) + j_1^2(u)]$ with $2j_0^2(u)$. This simplification correctly captures the amplitudes but *not* the phases of oscillation. The same argument applies in the case of Eq. (5.9) where the phases of oscillations are however controlled by the combination $[j_1^2(u)+j_2^2(u)]$. All in all the estimate of $\Omega_{gw}(k,\tau)$ inside the Hubble radius follows from Eq. (5.6) in the limit $k^2 P_T(k,\tau) \simeq Q_T(k,\tau)$ so that, at the very end, the spectral energy density in critical units becomes:

$$\Omega_{gw}(k,\tau) = \frac{k^2}{12\,H^2 a^2}\,P_T(k,\tau), \qquad k \gg a\,H,\tag{5.10}$$

which coincides with Eq. (5.1). Equation (5.10) is grossly correct for typical wavelength smaller than the Hubble radius (i.e. $k \gg a\,H$). But Eq. (5.10) *does not* correctly reproduce the phases of the spectral energy density when the corresponding wavelengths are both shorter and larger than the Hubble radius. The results of Eqs. (5.8) and (5.9) are illustrated in Fig. 2. The left plot of Fig. 2 should be compared with the left plot of Fig. 1: we clearly see that, in the limit $u > 1$ the oscillations are suppressed in comparison with the evaluation based on Eq. (5.1). The horizontal line in both plots illustrates $\overline{P}_T^{(r)}/24$.

It is finally useful to stress that the results discussed in this section do not apply at the present time, as already mentioned in connection with Eqs. (5.2)–(5.3). On the contrary the obtained results apply in the ranges defined by their respective arguments. As a general comment the spectral energy density at the present epoch is more suppressed by a factor that may range between 10^{-5} and 10^{-7} (see, for instance, [52]). This suppression is not only due to the redshift but also various damping sources including the neutron free streaming [67–70], the evolution of the relativistic species and the transition to the dominance of dark energy [17]. All these effect, however, are beyond the scope of the present discussion even if they may be crucial for a faithful assessment of the non-stationary features (especially over intermediate and high-frequencies) in concrete experimental situations.

5.3 Complementary considerations

The different definitions of the energy density of gravitational waves [71,72] stem directly from the equivalence principle that forbids the localization of the momentum of the gravitational field itself [66]. The same statement obviously holds for the pressure and the anisotropic stress of the gravitational waves. Since the energy-momentum tensor of the gravitational waves does not have a unique gauge-invariant (and frame-invariant) expression, through the years various expressions for the energy-momentum pseudo-tensor of the gravitational field have been deduced and they all lead to slightly different expressions of the energy density. Among them we may quote the Landau-Lifshitz approach [73–76], the Brill-Hartle strategy [77],

the Isaacson pseudotensor [78, 79]. In this analysis we privileged the Ford-Parker energy-momentum tensor [3] which is well defined both inside and outside the Hubble radius and it never leads to a violation of the energy conditions [66]. Other slightly different approaches have been pursued in the literature [80–84].

The purpose of this final subsection is to stress that the suppression of the non-stationary features associated with the spectral energy density of the relic gravitons does not depend on the specific form of the pseudo-tensor. The same kind of exercise discussed here can be repeated with all the various forms of the energy-momentum pseudo-tensor analyzed in Ref. [66]. To give a swift example we then consider the explicit form of the Landau-Lifshitz pseudo-tensor which is defined from the second-order fluctuations of the Einstein tensor [73–75] and its explicit form for a conformally flat metric $\overline{g}_{\mu\nu} = a^2(\tau)\eta_{\mu\nu}$ is given by:

$$\overline{\rho}_{gw} = \frac{1}{8a^2\ell_P^2}\left[8\mathscr{H}\,\partial_\tau h_{ij}\,h^{ij} + \left(\partial_m h_{ij}\,\partial^m h^{ij} + \partial_\tau h_{ij}\,\partial_\tau h^{ij}\right)\right]. \tag{5.11}$$

If we now compare the expression of $\rho_{gw}(\vec{x}, \tau)$ given in Eq. (5.5) with the one of $\overline{\rho}_{gw}(\vec{x}, \tau)$ we see that the difference is given by the first term inside the square bracket of Eq. (5.11). This term leads to a computable difference in the averaged energy density which is now given by

$$\langle\overline{\rho}_{gw}(\vec{x}, \tau)\rangle = \langle\rho_{gw}(\vec{x}, \tau)\rangle + \frac{2\mathscr{H}}{\pi^2\,a^2}\int k^2\,dk(G_k F_k^* + G_k^* F_k). \tag{5.12}$$

As a consequence the spectral energy density in critical units will be different in the various expanding stages. In particular during a radiation-dominated stage of expansion we have that the spectral energy density $\overline{\Omega}_{gw}(k, u)$ is:

$$\overline{\Omega}_{gw}(k, u) = \frac{\overline{P}_T^{(r)}}{24}\left(1 - \frac{7\sin^2 u}{u^2} + 3\frac{\sin 2u}{u}\right). \tag{5.13}$$

If we now compare Eq. (5.13) with Eq. (5.7) we see that the last two terms inside the squared brackets have different coefficients. These terms, however, do not change the relevant conclusion of our discussion namely the absence of a dominant oscillating term. Furthermore it turns out that the oscillating contributions are also suppressed as the wavelengths get shorter than the Hubble radius.

The comparison between the results of Eq. (5.7) and (5.13) is illustrated graphically in the left plot of Fig. 3. We restricted the interval of u to make the plot more readable; the curve with the largest amplitude of oscillation corresponds to the Landau-Lifshitz choice leading to Eq. (5.13). The curve with a smaller amplitude of oscillation corresponds follows from Eq. (5.7). In both cases, as expected, the oscillating contributions are suppressed in the limit $u > 1$. The same analysis leading to the comparison of Eqs. (5.7) and (5.13) is now illustrated in the case of a dust-dominated evolution where $\overline{\Omega}_{gw}(k, u)$ can be written as:

$$\overline{\Omega}_{gw}(v) = \frac{3\overline{P}_T^{(r)}}{32\,v^2}\left(1 - 6\frac{\sin 2v}{v} - \frac{14 + 25\cos 2v}{v^2} + 39\frac{\sin 2v}{v^3} - 39\frac{\sin^2 v}{v^4}\right). \tag{5.14}$$

The comparison of Eqs. (5.9) and (5.14) suggests once more that the coefficients of the terms appearing inside the squared bracket are different in the two cases even if the main physical conclusions are not modified since the oscillations are always suppressed in the limit $v > 1$. In the right plot of Fig. 3 the results of Eqs. (5.9) and (5.14) are graphically compared. The curve with the largest oscillatory amplitude corresponds to the Landau-Lifshitz pseudo-tensor. In both cases, however, the oscillations are suppressed in the limit $v > 1$ and this behaviour is crucially different from the one illustrated in Fig. 1. The comparison shows that the oscillations appearing in Fig. 1 are only caused by the approximation method and not by the dynamical evolution which is accurately described in terms of the spectral energy density.

5.4 Some other variables and their quasi-stationary limits

Having established that the spectral energy density is a quasi-stationary variable, it is natural to consider other variables whose oscillations may also be potentially large. If we consider, for instance, the tensor power spectrum and the chirp amplitude we see that they are strongly oscillating functions when the wavelengths are shorter than the Hubble radius. For concrete estimates the oscillations are arbitrarily averaged and often disregarded. This heuristic approach can be improved by using the spectral energy density as pivotal variable: in this way the oscillations of all the other observables will be automatically smeared inside the Hubble radius. Consider, as an example, the radiation-dominated stage; in this case we have that the exact evaluation of $\Omega_{gw}(k, u)$ leads directly to Eq. (5.7). If we are now interested in the tensor power spectrum inside the Hubble radius (or in the chirp amplitude) we have

$$P_T(k, u) = \frac{\overline{P}_T^{(r)}}{2\, u^2}\left(1 + 3\frac{\sin 2u}{u} - 7\frac{\sin^2 u}{u^2}\right), \tag{5.15}$$

$$h_c(k, u) = \frac{\sqrt{\overline{P}_T^{(r)}}}{2\, u}\sqrt{1 + 3\frac{\sin 2u}{u} - 7\frac{\sin^2 u}{u^2}}. \tag{5.16}$$

Equations (5.15)–(5.16) are only valid when all the relevant wavelengths are inside the Hubble radius, i.e. $u > 1$ and $k\tau > 1$. The same analysis can be repeated for a dust-dominated stage and in all other physical situations. One of the points of the present analysis has been that the spectral amplitude cannot be used for an explicit evaluation of the signal. We maintain this point since the spectral amplitude is defined, strictly speaking, only in the case of a process that is truly stationary. However if we really want to use, for some reason, $S_h(\nu)$ also in a non-stationary situation we can use the same logic leading to Eqs. (5.15)–(5.16): if we use the spectral energy density as pivotal variable we can always estimate

$$\nu\, S_h(|\nu|) = \lim_{k\tau \gg 1} \frac{12\, H^2\, a^2}{k^2}\, \Omega_{gw}(k, \tau). \tag{5.17}$$

In the case of a radiation-dominated stage this strategy simply leads to

$$\nu\, S_h(|\nu|) \to \frac{\overline{P}_T^{(r)}}{4\pi^2\nu^2\tau^2}\left[1 + \mathcal{O}\left(\frac{aH}{2\pi\nu}\right)\right]. \tag{5.18}$$

In Eq. (5.18) the contribution of the expansion is always present but the oscillating contributions disappear from the leading term. Equation (5.18) does not imply that the relic gravitons lead to a stationary process but the oscillating contributions are suppressed for wavelengths much smaller than the Hubble radius. Since these wavelengths correspond to frequencies that are much larger than the present expansion rate it is not necessary anymore to average by hand strongly oscillating trigonometric contributions. The considerations developed in this section are necessary for a sound construction of a template family for the relic graviton backgrounds. The potential signal must be accurately computed both in amplitude and slope since, as we showed, the shortcuts may enhance some of the spurious features that are simply related with the approximation methods. For the disambiguation between the relic and the late signals also the second-order correlation effects should be taken into due account [85, 86].

6 Concluding remarks

When the autocorrelation functions of stationary and ergodic ensembles of random fields are evaluated at different times τ_1 and τ_2 they ultimately depend on the difference $|\tau_1 - \tau_2|$. The gravitons produced quantum mechanically thanks to the early variation of the space-time curvature appear however from the inflationary vacuum with opposite comoving three-momenta. At the semiclassical level the quantum mechanical initial conditions represented by travelling waves turn into standing waves because of the evolution of the space-time curvature and this is why the diffuse backgrounds of relic gravitons are intrinsically non-stationary. The production of pairs with opposite momenta is then reflected into the standing oscillations that appear, with different features, in all the correlation functions and in the related observables. The lack of stationarity is reflected into the spectral energy density and in all the other observables that are customarily employed for the description of the relic signal. The first consequence of this observation is that the spectral amplitude cannot be used for a rigorous description of the signal since it is should be time-independent and determined, according to the Wiener-Khintchine theorem, by the Fourier transform of the autocorrelation function of the process. The non-stationary features of the diffuse backgrounds seem also reflected into the strong oscillations that characterize both the power spectra and the spectral energy density.

The analysis of the present paper shows however that the spectral energy density is only mildly non-stationary since the time dependence associated with $\Omega_{gw}(\nu, \tau)$ turns out to be strongly suppressed in the large-scale limit provided a consistent definition of the energy density is adopted. If, on the contrary, the spectral energy density is related to the tensor power spectrum within a more heuristic (but rather standard) perspective the oscillations dominate the leading terms. According to this second approximate strategy the spectral energy density and the tensor power spectrum are not related in general terms but only in the limit where all the comoving wavelengths are inside the Hubble radius at the present time. This investigation shows that the non-stationary nature of the process affects directly also the spectral energy density but in a much milder way which is furthermore suppressed in the large-scale limit.

If the spectral energy density is used as the pivotal variable the strong oscillations appearing in the power spectrum and in the chirp amplitude are smeared without assuming any ad hoc time average that is often employed in the description of the relic signal. For a direct evaluation of the spectral energy density the optimal strategy is instead to take the large-scale limit *after* evaluating all the power spectra in their exact form. While the lack of stationarity of the relic graviton backgrounds is reflected into the time-dependence of the spectral energy density, it is not true that the phases of oscillation of the tensor power spectrum are directly reflected in $\Omega_{gw}(\nu, \tau)$. The heuristic arguments suggesting that the phases of the spectral energy density and of the tensor power spectrum coincide has been clarified and partially refuted in this analysis. An accurate evaluation of the spectral energy density can be used to bridge the stationary and quasi-stationary descriptions of the relic gravitons. This means, in practice, that the relic signal cannot be simply identified by looking either at the slope or at the amplitude of a given observable. A naive viewpoint stipulates that the detection of the relic gravitons should be achieved with instruments built for general purposes and by only looking at some features of the signal as if a physical template family for the diffuse backgrounds was just optional. The ideas conveyed in this analysis show the opposite: while the spectral slopes of a stationary background may be confused with the relic gravitons, this cannot happen

if the slopes, the amplitudes and the correlation properties are concurrently analyzed in the construction of an appropriate non-stationary template. It is our opinion, as stressed in the past, that the template family should wisely include also the second-order correlation effects that are a direct consequence of the quantum origin of the relic signal.

Aknowledgements

A   Scalar random fields

A.1   Stationary processes

In the case of scalar random fields the autocorrelation function is introduced in full analogy with the case of the random functions discussed in section 2. In particular the autocorrelation function is be denoted as $\Gamma_\phi(\tau_1 - \tau_2)$ and it appears in the ensemble average of the scalar amplitudes:

$$\langle \phi(\widehat{k},\, \tau_1)\, \phi(\widehat{p},\, \tau_2) \rangle = \mathscr{C}_\phi\, \delta^{(2)}(\widehat{k} - \widehat{p})\, \Gamma_\phi(\tau_1 - \tau_2). \tag{A.1}$$

In Eq. (A.1) the numerical constant $\mathscr{C}_\phi$ fixes the relation between power spectrum and the spectral amplitude; $\delta^{(2)}(\widehat{k} - \widehat{k}') = \delta(\varphi - \varphi')\, \delta(\cos\vartheta - \cos\vartheta')$ is the angular delta function. From Eq. (A.1) the spectral amplitude is defined, in practice, as in the case of Eq. (2.3)

$$\phi(\widehat{k},\nu) = \int_{-\infty}^{\infty} d\tau\ e^{-2i\,\pi\nu\tau}\, \phi(\widehat{k},\tau), \qquad \langle \phi(\widehat{k},\nu)\, \phi(\widehat{p},\nu') \rangle = \mathscr{C}_\phi\, \delta(\nu + \nu')\, S_\phi(\nu)\, \delta^2(\widehat{k} - \widehat{p}). \tag{A.2}$$

The autocorrelation function $\Gamma_\phi(\tau_1 - \tau_2)$ and the spectral amplitude $S_\phi(\nu)$ are then related in a way similar to the one already established in Eq. (2.4):

$$S_\phi(\nu) = \int_{-\infty}^{+\infty} dz\, \Gamma_\phi(z)\, e^{2i\,\pi\,\nu\,z}. \tag{A.3}$$

From Eq. (A.3) we can also argue that to verify whether a given expression is the correlation function of a stationary random process we must find its Fourier transform and establish whether or not it is always positive semi-definite. Equation (A.3) explicitly illustrates that if $\Gamma(|\tau_1 - \tau_2|)$ is dimensionless $S_\phi(|\nu|)$ has dimensions of a time. In summary a scalar random field can therefore be represented in Fourier space as:

$$\phi(\vec{x},\tau) = \int_{-\infty}^{\infty} d\nu \int d\widehat{k}\ e^{2\,i\,\pi\,\nu\,(\tau - \widehat{k}\cdot\vec{x})}\ \phi(\nu,\widehat{k}), \tag{A.4}$$

where the angular integration is performed over $d\widehat{k} = d\cos\vartheta\, d\varphi$; if the field $\phi(\vec{x},\tau)$ is real (as we shall assume throughout this discussion) then $\phi^*(\nu,\widehat{k}) = \phi(-\nu,\widehat{k})$. Equations (A.2) and (A.4) are fully consistent the starting point of Eq. (A.1).

A.2   Homogeneous processes

An ensemble of scalar random fields described by Eqs. (A.2)–(A.4) and characterized by a stationary autocorrelation function is also homogeneous. To consider this point in more detail we may actually compute the correlation function for separated spatial locations and

$$\langle \phi(\vec{x},\tau_1)\, \phi(\vec{y},\tau_2) \rangle = 8\pi\mathscr{C}_\phi \int_0^{\infty} S_\phi(|\nu|)\, e^{2i\pi\nu\,(\tau_1 - \tau_2)}\, j_0(2\pi\,\nu\,r)\, d\nu, \tag{A.5}$$

and note that it always depends upon $r = |\vec{x} - \vec{y}|$. The result (A.5) follows from Eqs. (A.2) and (A.4); moreover, since $j_0(z)$ denotes the spherical Bessel function of zeroth order [60,61], the result of Eq. (A.5) is well defined not only for $\tau_1 \to \tau_2$ but also when $r \to 0$. A homogeneous random field can also be Fourier transformed in a slightly different manner, namely

$$\phi(\vec{x},\tau) = \frac{1}{(2\pi)^{3/2}} \int d^3k\ e^{-i\vec{k}\cdot\vec{x}}\, \overline{\phi}(\vec{k},\tau), \qquad \overline{\phi}^*(\vec{k},\tau) = \overline{\phi}(-\vec{k},\tau). \tag{A.6}$$

If the stationarity of the process is disregarded, an ensemble of homogeneous scalar random fields must also obey

$$\langle \overline{\phi}(\vec{k}, \tau)\, \overline{\phi}(\vec{p}, \tau) \rangle = \frac{2\pi^2}{k^3}\, \delta^{(3)}(\vec{k} + \vec{p})\, P_\phi(k, \tau), \tag{A.7}$$

where $P_\phi(k, \tau)$ denotes, in the present notations, the scalar power spectrum; as anticipated $P_\phi(k, \tau)$ (unlike the spectral amplitude) is always dimensionless. Equations (A.6)–(A.7) do not assume the stationarity of the process but since Eqs. (A.4) and (A.7) are both valid Fourier representations of an ensemble of scalar random fields the two can be related. For this purpose we preliminarily compute from Eqs. (A.6)–(A.7) the analog of Eq. (A.5) valid in the case $\tau_1 \to \tau_2 = \tau$:

$$\langle \phi(\vec{x}, \tau)\, \phi(\vec{y}, \tau) \rangle = \int_0^\infty \frac{dk}{k}\, P_\phi(k, \tau)\, j_0(k\, r), \tag{A.8}$$

where, as before, $r = |\vec{x} - \vec{y}|$. Thus Eqs. (A.5) and (A.8) must coincide in the two concurrent limits $\tau_1 \to \tau_2$ and $r \to 0$

$$8\pi \mathscr{C}_\phi \int_0^\infty S_\phi(|\nu|)\, d\nu = \int_0^\infty \frac{dk}{k}\, P_\phi(k, \tau). \tag{A.9}$$

Equation (A.9) implies that by arranging the numerical factor C_ϕ the spectral amplitude and the power spectrum coincide

$$\nu\, S_\phi(|\nu|) = P_\phi(|\nu|), \qquad 8\pi \mathscr{C}_\phi = 1. \tag{A.10}$$

provided $P_\phi(k, \tau)$ *does not have an explicit time dependence*. The tensor analog of Eq. (A.10) is given in Eq. (2.16) ad the numerical difference between the two conditions is only due to the sum over the tensor polarizations. According to Eq. (A.10) the connection between the power spectrum and the spectral amplitude is only well defined in the stationary case. On the other hand, if the process is only homogeneous (but not necessarily stationary) the power spectrum is always well defined but does not lead to an autocorrelation function that depends only on $(\tau_1 - \tau_2)$.

B   Transition matrices and their limits

The elements of the transition matrix associated with a radiation dominated evolution are given by:

$$A_{f\,f}^{(r)}(u, u_r) = \cos(u - u_r) + \frac{\sin(u - u_r)}{u_r},$$

$$A_{f\,g}^{(r)}(u, u_r) = \sin(u - u_r),$$

$$A_{g\,f}^{(r)}(u, u_r) = \left(\frac{1}{u_r} - \frac{1}{u}\right)\cos(u - u_r) - \left(1 + \frac{1}{u\,u_r}\right)\sin(u - u_r),$$

$$A_{g\,g}^{(r)}(u, u_r) = \cos(u - u_r) - \frac{\sin(u - u_r)}{u}, \tag{B.1}$$

where $u(\tau)$ has been introduced already in Eq. (4.1) and, by definition, $u_r = u(-\tau_r)$. We furthermore note that $(u - u_r) = (\tau + \tau_r)$ and in the limit $\tau \to -\tau_r$ the off-diagonal terms of the transition matrix vanish while the diagonal ones tend to 1. Deep in the radiation stage (i.e. $u \gg u_r$) the various entries of the transition matrix can also be expanded for $|u_r| \ll 1$ and, in this limit, Eq. (B.1) becomes:

$$A_{f\,f}^{(r)}(u, u_r) = \left(\frac{u}{u_r}\right) j_0(u) + \frac{u\, u_r}{2} j_0(u) + \mathcal{O}(|u_r|^2),$$

$$A^{(r)}_{fg}(u,\,u_r) = \sin u - u_r \cos u + \mathcal{O}(|u_r|^2),$$

$$A^{(r)}_{gf}(u,\,u_r) = -\left(\frac{u}{u_r}\right) j_1(u) - \frac{u\,u_r}{2} j_1(u) + \mathcal{O}(|u_r|^2),$$

$$A^{(r)}_{gg}(u,\,u_r) = -u\,j_1(u) - u\,y_1(u) + \mathcal{O}(|u_r|^2), \tag{B.2}$$

where $j_n(z)$ and $y_n(z)$ are the standard spherical Bessel functions of index n and argument z. The spherical Hankel functions of first and second kind [60,61] are instead defined, respectively, as $h_n^{(1)}(z) = j_n(z) + i\,y_n(z)$ and as $h_n^{(2)}(z) = j_n(z) - i\,y_n(z)$. The transition matrix associated with the matter-dominated phase can be swiftly expressed in terms of the spherical Hankel functions:

$$A^{(m)}_{ff}(v,\,v_{eq}) = \frac{i}{2} v\,v_{eq} \left[h_2^{(1)}(v_{eq})\,h_1^{(2)}(v) - h_2^{(2)}(v_{eq})h_1^{(1)}(v) \right],$$

$$A^{(m)}_{fg}(v,\,v_{eq}) = \frac{i}{2} v\,v_{eq} \left[h_1^{(1)}(v_{eq})\,h_1^{(2)}(v) - h_1^{(2)}(v_{eq})h_1^{(1)}(v) \right],$$

$$A^{(m)}_{gf}(v,\,v_{eq}) = \frac{i}{2} v\,v_{eq} \left[h_2^{(2)}(v_{eq})\,h_2^{(1)}(v) - h_2^{(1)}(v_{eq})h_2^{(2)}(v) \right],$$

$$A^{(m)}_{gg}(v,\,v_{eq}) = \frac{i}{2} v\,v_{eq} \left[h_1^{(2)}(v_{eq})\,h_2^{(1)}(v) - h_1^{(1)}(v_{eq})h_2^{(2)}(v) \right], \tag{B.3}$$

where the dimensionless variable $v(\tau)$ has been defined in Eq. (4.11); moreover, by definition, $v_{eq} = v(\tau_{eq})$. As before the entries of the transition matrix given in Eq. (B.3) are all real. It can be immediately appreciated that in the limit $v \to v_{eq}$ the diagonal terms of the matrix go to 1 while the two off-diagonal contributions vanish. During the matter-dominated epoch the results of Eq. (B.3) can be expanded in the limit $|v_{eq}| \ll 1$ and the explicit results become:

$$A^{(m)}_{ff}(v,\,v_{eq}) = 3\left(\frac{v}{v_{eq}^2}\right) j_1(v) + \frac{v}{2} j_1(v) + \mathcal{O}(|v_{eq}|^2),$$

$$A^{(m)}_{fg}(v,\,v_{eq}) = 3\left(\frac{v}{v_{eq}}\right) j_1(v) + \frac{v\,v_{eq}}{2} j_1(v) + \mathcal{O}(|v_{eq}|^2),$$

$$A^{(m)}_{gf}(v,\,v_{eq}) = -3\left(\frac{v}{v_{eq}^2}\right) j_2(v) - \frac{v}{2} j_2(v) + \mathcal{O}(|v_{eq}|^2),$$

$$A^{(m)}_{gg}(v,\,v_{eq}) = -\left(\frac{v}{v_{eq}}\right) j_2(v) - \frac{v\,v_{eq}}{2} j_2(v) + \mathcal{O}(|v_{eq}|^2). \tag{B.4}$$

Both in the case of Eqs. (B.1) and (B.4) the commutation relations imply that the transition matrices must be unitary so that, in particular, $A^{(X)}_{ff} A^{(X)}_{gg} - A^{(X)}_{fg} A^{(X)}_{gf} = 1$ where $X = r,\,m$ and the various entries are all functions of their respective arguments in each of the corresponding stages; see also, in this respect, Eq. (4.4) and the discussion therein.

References

[1] L. P. Grishchuk, Sov. Phys. JETP **40**, 409 (1975) [Zh. Eksp. Teor. Fiz. **67**, 825 (1974)].

[2] L. P. Grishchuk, Annals N. Y. Acad. Sci. **302**, 439 (1977).

[3] L. H. Ford and L. Parker, Phys. Rev. **D16**, 1601 (1977).

[4] B. L. Hu and L. Parker, Phys. Lett. A **63**, 217 (1977).

[5] A. D. Sakharov, Sov. Phys. JETP **22**, 241 (1966) [Zh. Eksp. Teor. Fiz. **49**, 345 (1965)].

[6] P. J. E. Peebles and J. T. Yu, Astrophys. J. **162** 815 (1970).

[7] R. A. Sunyaev and Y. B. Zeldovich, Astrophys. Space Sci. **7**, 3 (1970).

[8] A. A. Starobinsky, JETP Lett. **30**, 682 (1979) [Pis'ma Zh. Eksp. Teor. Fiz. **30**, 719 (1979)].

[9] L. F. Abbott and M. B. Wise, Nucl. Phys. B **244**, 541 (1984).

[10] S. W. Hawking, Phys. Lett. **150B**, 339 (1985).

[11] V. A. Rubakov, M. V. Sazhin, and A. V. Veryaskin, Phys. Lett. B **115**, 189 (1982).

[12] R. Fabbri and M. d. Pollock, Phys. Lett. **125B**, 445 (1983).

[13] Y. Akrami *et al.* [Planck Collaboration], Astron. Astrophys. **641**, A10 (2020).

[14] N. Aghanim *et al.* [Planck Collaboration], Astron. Astrophys. **641**, A6 (2020).

[15] P. A. R. Ade *et al.* [BICEP and Keck], Phys. Rev. Lett. **127**, 151301 (2021).

[16] M. Giovannini, Phys. Rev. D **58**, 083504 (1998); Phys. Rev. D **60**, 123511 (1999); Class. Quant. Grav. **16**, 2905 (1999).

[17] M. Giovannini, Prog. Part. Nucl. Phys. **112**, 103774 (2020).

[18] D. J. Reardon, *et al.*, Astrophys. J. Lett. **951**, L6 (2023)

[19] G. Agazie *et al.* [NANOGrav], Astrophys. J. Lett. **951**, L8 (2023).

[20] J. Antoniadis *et al.* [EPTA and InPTA] Astron. Astrophys. **678**, A50 (2023).

[21] H. Xu, S. Chen, *et al.* Res. Astron. Astrophys. **23**, 075024 (2023).

[22] B. P. Abbott *et al.* [LIGO Scientific and Virgo], Phys. Rev. D **100**, 061101 (2019).

[23] R. Abbott *et al.* [KAGRA, Virgo and LIGO Scientific collaboration], Phys. Rev. D **104**, 022004 (2021).

[24] M. V. Sazhin, Sov. Astron. **22**, 36 (1978) [Astron. Zh. **55**, 65 (1979)].

[25] S. Detweiler, Astrophys. J. **234**, 1100 (1979).

[26] R. W. Hellings and G. S. Downs, Astrophys. J. Lett. **265** L39 (1983).

[27] V. M. Kaspi, J. H. Taylor, and M. F. Ryba, Astrophys. J. **428**, 713 (1994).

[28] F. A. Jenet *et al.*, Astrophys. J. **653**, 1571 (2006).

[29] Z. Arzoumanian *et al.*, Astrophys. J. Lett. **905**, L34 (2020).

[30] B. Goncharov *et al.* Astrophys. J. Lett. **917**, L19 (2021).

[31] S. Chen, *et al.* Mon. Not. Roy. Astron. Soc. **508**, 4970 (2021).

[32] J. Antoniadis, *et al.* Mon. Not. Roy. Astron. Soc. **510**, 4873 (2022).

[33] V. F. Schwartzmann, JETP Lett. **9**, 184 (1969).

[34] M. Giovannini, H. Kurki-Suonio and E. Sihvola, Phys. Rev. D **66**, 043504 (2002).

[35] R. H. Cyburt, B. D. Fields, K. A. Olive, and E. Skillman, Astropart. Phys. **23**, 313 (2005).

[36] E. Jacopini, F. Pegoraro, E. Picasso, and L. Radicati, Phy. Lett. **73**, 140 (1979).

[37] C. Reece, P. Reiner, and A. Melissinos, Phys. Lett. A **104**, 341 (1984).

[38] C. Reece, P. Reiner, and A. Melissinos, Nucl. Inst. and Methods, A **245**, 299 (1986).

[39] Ph. Bernard, G. Gemme, R. Parodi and E. Picasso, Rev. Sci. Instrum. **72**, 2428 (2001).

[40] R. Ballantini, P. Bernard, A. Chincarini, G. Gemme, R. Parodi and E. Picasso, Class. Quant. Grav. **21**, S1241 (2004).

[41] A. M. Cruise, Mon. Not. R. Astron. Soc. **204**, 485 (1983); Class. Quantum Grav. **17** , 2525 (2000); A. M. Cruise and R. Ingley, Class. Quantum Grav. **23**, 6185 (2006).

[42] A. M. Cruise and R. M. Ingley, Class. Quantum Grav. **22**, S479 (2005).

[43] F. Li, M. Tang and D. Shi, Phys. Rev. D **67**, 104008 (2003).

[44] F. Li, Z. Wu and Y. Zhang, Chin. Phys. Lett. **20**, 1917 (2003).

[45] A. Nishizawa *et al.*, Phys. Rev. D **77**, 022002 (2008).

[46] A. T. Akutsu *et al.*, Phys. Rev. Lett. **101**, 101101 (2008).

[47] M. Giovannini, JCAP **05**, 056 (2023).

[48] C. W. Gardiner, *Handbook of stochastic methods*, (Springer-Verlag, Berlin, 1987).

[49] S. Karlin and H. M. Taylor, *A first course in stochastic processes* (Academic Press, New York, 1975).

[50] N. Wiener, Acta Math. **55** (1930).

[51] A. Khintchine, Math. Ann. **104**, 415 (1931).

[52] M. Giovannini, *Relic Gravitons* (World Scientific, Singapore, 2024).

[53] P. Michelson, Mon. Not. Roy. Astron. Soc. **227**, 933 (1987).

[54] N. Christensen, Phys. Rev. D **46**, 5250 (1992).

[55] E. Flanagan ,Phys. Rev. D **48**, 2389 (1993)

[56] D. Babusci and M. Giovannini, Phys. Rev. D **60**, 083511 (1999).

[57] B. Allen, E. E. Flanagan and M. A. Papa, Phys. Rev. D **61**, 024024 (2000).

[58] L. P. Grishchuk, Usp. Fiz. Nauk **182**, 222 (2012).

[59] N. Christensen, Rep. Prog. Phys. **82**, 016903 (2019).

[60] A. Erdelyi, W. Magnus, F. Oberhettinger, and F. R. Tricomi *Higher Trascendental Functions* (Mc Graw-Hill, New York, 1953).

[61] M. Abramowitz and I. A. Stegun, *Handbook of Mathematical Functions* (Dover, New York, 1972).

[62] M. Giovannini, Phys. Rev. D **108**, 123508 (2023)

[63] M. S. Turner, M. J. White and J. E. Lidsey, Phys. Rev. D **48**, 4613 (1993).

[64] S. Chongchitnan and G. Efstathiou, Phys. Rev. D **73**, 083511 (2006).

[65] M. Giovannini, Phys. Lett. B **668**, 44 (2008); Class. Quant. Grav. **26**, 045004 (2009).

[66] M. Giovannini, Phys. Rev. D **100**, 083531 (2019).

[67] S. Weinberg, Phys. Rev. D **69**, 023503 (2004).

[68] D. A. Dicus and W. W. Repko, Phys. Rev. D **72**, 088302 (2005).

[69] H. X. Miao and Y. Zhang, Phys. Rev. D **75**, 104009 (2007).

[70] B. A. Stefanek and W. W. Repko, Phys. Rev. D **88**, 083536 (2013).

[71] C. W. Misner, K. S. Thorne, and J. A. Wheeler, *Gravitation* (Freeman, New York, 1973).

[72] S. Weinberg, *Gravitation and Cosmology*, (Wiley, New York, 1972).

[73] L. D. Landau and E. M. Lifshitz, *The Classical Theory of Fields*, (Pergamon Press, New York, 1971).

[74] L. R. Abramo, Phys Rev. D **60**, 064004 (1999).

[75] M. Giovannini, Phys. Rev. D **73**, 083505 (2006); Phys. Rev. D **91**, 023521 (2015).

[76] D. Su and Y. Zhang, Phys. Rev. D **85**, 104012 (2012).

[77] D. R. Brill and J. B. Hartle, Phys. Rev. **135**, B271 (1964).

[78] R. A. Isaacson, Phys. Rev. **166**, 1263 (1968); Phys. Rev. **166**, 1272 (1968).

[79] M. A. H. MacCallum and A. H. Taub, Commun. Math. Phys. **30**, 153 (1973).

[80] L. C. Stein and N. Yunes, Phys. Rev. D **83**, 064038 (2011).

[81] M. Isi and L. C. Stein, Phys. Rev. D **98**, 104025 (2018).

[82] S. V. Babak and L. P. Grishchuk, Phys. Rev. D **61**, 024038 (2000).

[83] L. M. Butcher, A. Lasenby and M. Hobson, Phys. Rev. D **78**, 064034 (2008).

[84] L. M. Butcher, M. Hobson and A. Lasenby, Phys. Rev. D **86**, 084012 (2012).

[85] M. Giovannini, Phys. Rev. D **83**, 023515 (2011); Class. Quant. Grav. **34**, 035019 (2017).

[86] M. Giovannini, Mod. Phys. Lett. A **32**, 1750191 (2017); Phys. Rev. D **99**, 123507 (2019).